PLASTIC STRAIN IN MATERIALS

UNDER THE INFLUENCE OF IMPULSIVE LOAD

PLASTIC STRAIN IN MATERIALS

UNDER THE INFLUENCE OF IMPULSIVE LOAD

BY

S. K. SINHA

A Thesis

Submitted to the Faculty of Graduate Studies

in Partial Fulfilment of the Requirements

for the Degree

Master of Engineering

McMaster University

May, 1968

MASTER OF ENGINEERING
(Mechanical Engineering)

McMASTER UNIVERSITY
Hamilton, Ontario.

TITLE: Plastic Strain in Materials Under The Influence of Impulsive Load

AUTHOR: Shailendra Kumar Sinha, B.Sc. Eng. (Mech.), Ranchi University, India.

SUPERVISOR: Dr. G. Kardos

NUMBER OF PAGES: xiii, 89

SCOPE AND CONTENT:

Equipment was designed for testing dynamic behaviour of materials subjected to impulsive load.

Detail design of the equipment and experimental techniques have been described.

Armco Ingot Iron with 99.8% purity was tested. Before testing, the material was fully annealled.

"n" and "$G(\varepsilon,t)$ (as occurring in the characteristic equation σ_m^n to $K(n) = G(\varepsilon,t)$, for this material were evaluated.

The material was found to ber very sensitive to strain rates.

ACKNOWLEDGEMENTS

The author wishes to express his sincere thanks to Dr. G. Kardos for his continuous encouragement and advice in the course of the present work. The complete freedom, that he offered in the designing of the equipment, is much appreciated.

The author feels highly indebted to Mr. R. Brown and Mr. J. Crookes, the technicians of the department, for their valuable help and suggestions in the installation and operation of the equipment.

The author is thankful to the workers of the Machine Shop of McMaster University, for preparing the parts of latching and release mechanisms and the samples for the present test.

The author is obliged to the Department of Mechanical Engineering for the support of his finances without which the present work could not have been possible.

Thanks are also due to the author's colleagues for their help in various ways.

Finally, the author thanks Mrs. Anne Woodrow for her care in the typing of the present dissertation.

The present work was supported under N.R.C. Grant No. 214-1354-000.

ABSTRACT

Equipment was designed for testing the dynamic behaviour of materials subjected to impulsive load. It consisted of a Drop Table, a Hydraulic Intensifier and some accessories necessary for fulfilling the conditions of a single blow. The load applied to the material was recorded on an oscilloscope through a strain gauge load cell.

The minimum duration of loading with this equipment was found to be 18 milliseconds. Peak stresses as high as 300,000 p.s.i. can be readily produced by the equipment. The drop height of the table ranges from 2-1/2" to 60".

Dynamic stress tests were carried out on Armco Ingot Iron. Fully annealled samples were used. Annealling was done in two batches at the same temperature but with different soak durations. Static properties of the material were determined for comparison purposes. The material was found to be strain rate sensitive. The batch which was annealled for the longer period was found to be the more sensitive.

The material properties, "n" and "G" (ϵ_p, t) (the stress dislocation velocity exponent and the flow function), occurring in the characteristic equation $\sigma_m^n \, t_o \, K(n) = G(\epsilon_p, t)$, as proposed by Kardos [11], for the present material were evaluated. The average value of "n" was found to be equal to 5 and 6 for the two batches respectively.

The present equipment can be used for establishing these material properties for any material.

TABLE OF CONTENTS

III. TABLES

NOTATIONS

a	an exponent
b	Burger's Vector
C	a constant
ε_E	elastic strain
ε_p	plastic strain
ε_T	total strain
$\dot{\varepsilon}$	$\frac{dE}{dt}$ = rate of strain
ε_V	volumetric strain
E	Young's Modulus of Elasticity
F	any applied force
f	a fractional number
k	stiffness of the spring
K	Boltzman's Constant
K'	Bulk Modulus of Elasticity of Oil
L	length of a mobile dislocation
n	a material constant known as Stress Dislocation Velocity Exponent
α	a material constant
t_o	duration of loading
t_d	delay time
t_m	mean time before a dislocation is released
p	pressure in the oil chamber

m	mass of the drop table assembly
T	absolute temperature
U	activation energy
ν	velocity of dislocation
$f(t)$	a time dependent function
σ	applied stress
σo	lower yield stress
σm	peak stress
$\Delta\sigma$	amount of stress used in overcoming strain hardening
τ	applied shear stress
τo	a proportionality constant
$H(\epsilon_p)$	flow function
$G(\epsilon_p, t_o)$	flow function corrected for strain hardening
V	volume of oil in the oil chamber
$K(n)$	form factor
q	strain hardening co-efficient
ϕ	time ratio t/to
ρ	dislocation density
ρ_o	density of grown-in dislocations
h	height of drop table
dx	small displacement
dV	small change in the volume of oil
A	area of drive piston

W	weight of the table
M	a moment
P	a force

LIST OF ILLUSTRATIONS

CHAPTER 1

INTRODUCTION

1.1 Brief History of Dynamic Loading

It is a well known fact that materials behave differently when subjected to dynamic loads than to static loads. This was first realized by Hopkinson [1] in 1872. While studying the propagation of stress waves in solids, he noticed that the rupture stress of the material was much higher than that predicted by static tests (this discovery was accidental and he did not go into much detail). Davis [2] proved this fact experimentally in 1938.

Manjoine [3] carried out extensive tests on mild steel samples with different rates of strain. He concluded that the yield stress and the ultimate stress of mild steel increase with the increase in the rate of loading. He also considered the effects of temperature by testing the samples at different temperatures and concluded that with an increase in temperature there is a decrease in the yield and ultimate stresses.

Clark and Wood [4], while studying the dynamic behaviour of mild steel, found that the material required a definite time to yield after any stress higher than its yield stress had been applied. This they called "Delay Time". They tried to find a relationship between the delay time and the applied stress and suggested the following empirical relation:

$$t_d = 4 \times 10^{-4} \times \left(\frac{\sigma - \sigma_0}{\sigma_0} \right)^{-6} \text{ secs.} \qquad (1.1.1)$$

where,

t_d = the delay time,

σ = applied stress,

σ_o = lower yield stress.

From this equation, it should be noted that the delay time would be very long if the difference between the applied stress and the yield stress was small. Table 1 of Appendix III illustrates this point by showing the relation between the delay time and the applied stress for some typical applied stress values.

The Table shows that if a stress, 50% greater than the lower yield stress of the material, is applied for a duration of less than 25 milliseconds (less than the required time for the initiation of plastic strain), the material will not show any permanent deformation. In other words, if the duration of loading be less than 25 milliseconds, then we can safely load it to a stress 50% greater than the lower yield stress. This indicates that for loads of short duration the design stress should be equal to or greater than the static yield stress - which is not the case in current design practice.

The above theory was further verified by Clark [5] in 1954. Samples of mild steel were loaded very rapidly beyond the yield stress and the load was held constant for a period equal to 3/5th of the

corresponding delay time. The load was then removed. The samples showed no apparent yield. The specimens were again loaded and it was found that the delay time had decreased to 2/5th of the original value.

In addition, if the applied stress is greater than the lower yield stress and the duration of loading is greater than the corresponding delay time, the permanent strain will not necessarily reach the values expected from static tests. The plastic flow itself takes place in a finite time which must be added to the delay time.

In design the problem is to determine the stress level and the stress duration to which a component can be subjected without affecting its functioning.

1.2 Plastic Flow

It is well established [6] that plastic strain is related to the movement of dislocations within the material. These dislocations may be either grown-in dislocations or dislocations generated by various mechanisms. When a stress is applied, the dislocations move in the direction of the stress and cause plastic strain. Forward movement of the dislocations is restricted as obstacles are encountered and these must be overcome for further movement to occur. Part of the stress is used in overcoming these obstacles and the net stress available for the movement of the dislocations is therefore less than the total stress, and, the actual deformation is less than the nominal.

If the strained material is left for some time under load, the dislocations rearrange themselves in positions of minimum energy. Some of them escape by means of cross-slip or glide. The net effect is an increase in plastic strain and a decrease in the stress. This is known as relaxation and the time required for the relaxation is known as the relaxation time.

In the case of static loading, the rate of loading is very slow compared to the relaxation time of the material. The material is simultaneously relaxing, and the plastic strain is therefore quite large. Whereas, in the case of dynamic loading, the rate of loading is quite high and the material cannot relax completely. As a result, the total plastic strain is less. If the load is removed before the material has relaxed completely, then there is no driving force to make the dislocations move further. Therefore, the plastic stress stops on the removal of the load. For this reason, the actual plastic strain is far less in the case of dynamic loading than in the case of static loading of the same material under the same load.

It is clear that the amount of plastic strain is proportional to the total movement of the dislocations during the period of loading. In other words, the total plastic strain is proportional to the product of the velocity of dislocations and the duration of loading.

Campbell [7] has derived a mathematical model for the yield criterion of any material based on the concept of the release of dislocations from pinning.

1.3 Campbell's Yield Criterion

The mean time necessary for a dislocation to be released from its atmosphere is given by,

$$t_m \propto e^{U/KT} \tag{1.3.1}$$

where,

t_m = Mean Time

U = Activation Energy

K = Boltzmann's Constant

T = Absolute Temperature

Therefore, the number of dislocations released in time t is proportional to the integral,

$$\int_0^t e^{-U/KT}\, dt \tag{1.3.2}$$

Using Yokobori's approximation [8] for activation energy as a function of applied stress,

$$U = \frac{1}{\alpha} \ln(\sigma/\sigma_o) \tag{1.3.3}$$

where,

α = a constant

σ = applied stress

σ_o = lower yield stress

we find that,

$$e^{-U/KT} = (\sigma/\sigma_0)^n \tag{1.3.4}$$

where,

$$n = \frac{1}{\alpha KT}$$

Campbell concludes that a material starts to yield at a time t when,

$$\int_0^t (\sigma/\sigma_0)^n \, dt = C \tag{1.3.5}$$

where,

C = the number of dislocations released to give perceptible yield.

1.4 Hahn's Model Equation for Dynamic Yielding

Hanh [9] derived an expression for total strain from a consideration of the movement of dislocations. Total strain is equal to the sum of the elastic and plastic strains. The plastic strain is given by the relation,

$$\dot{\epsilon}_p = 0.5\,bLv \tag{1.4.1}$$

where,

b = Burger's vector,

L = Length of mobile dislocations,

v = velocity of dislocations

The length of mobile dislocations is proportional to the dislocation density which in turn can be approximated to the plastic strain by some exponential relation. Thus,

$$L \simeq f\rho \tag{1.4.2}$$

and

$$\rho = \rho_0 + c\,\epsilon_p^{a} \tag{1.4.3}$$

where,

ρ = dislocation density,

ρ_0 = density of the grown-in dislocations

a,c,f = some constants

The velocity of dislocations can be approximated to the applied stress by another exponential law as proposed by Gilman and Johnston [10] as,

$$V = \left[\frac{\sigma - \Delta\sigma}{2\tau_0}\right]^{n} \tag{1.4.4}$$

where,

n = a constant,

τ_0 = proportionality constant,

$\Delta\sigma$ = amount of stress used in overcoming strain hardening.

The total strain can, therefore, be expressed as,

$$\dot{\epsilon}_T = \frac{\dot{\sigma}}{E} + 0.5\, b f \rho_0 \left(1 + c\,\epsilon_p^a/\rho_0\right)\left(\frac{\sigma - \Delta\sigma}{2\tau_0}\right)^n \qquad (1.4.5)$$

where,

E = Young's Modulus of Elasticity

If the stress function and the material constants are known, this equation may be used to calculate the total strain in any material.

1.5 Kardos's Simplifications and the New Design Equation

In practice, it is very difficult to calculate the large number of constants appearing in Hahn's Model Equation. It is especially difficult to determine the grown-in dislocation density as this depends upon the complete past history of the material. Kardos [11] suggests that, instead of evaluating the constants individually, it is better to lump them together. The overall value of the constant can then be determined experimentally.

For large plastic strains, the contribution of the elastic strain is small and therefore the first term can be neglected. By rearranging the above equation so that all the constants and the plastic strain term are brought to one side, we get

$$\frac{(2\tau_0)^n}{0.5\, b f \rho_0 \left(1 + c\,\epsilon_p^a/\rho_0\right)}\, d\epsilon = (\sigma - \Delta\sigma)^n\, dt \qquad (1.5.1)$$

Integrating both sides we get,

$$\int_0^{\epsilon_0} \frac{(2\tau_0)^n}{0.5\, b f \rho_0 (1 + c\, \epsilon_p^a/\rho_0)}\, d\epsilon = \int_0^{t_0} (\sigma - \Delta\sigma)^n dt \qquad (1.5.2)$$

where,

ϵ_0 = final plastic strain,

t_0 = the duration of loading.

The integral on the left hand depends upon plastic strain (which is also known as the flow of the material). This he calls "Flow Function" and designates by capital H.

Thus,

$$H(\epsilon_p) = \int_0^{\epsilon_0} \frac{(2\tau_0)^n}{0.5\, b f \rho_0 (1 + c\, \epsilon_p^a/\rho_0)}\, d\epsilon \qquad (1.5.3)$$

The right hand side can be written as,

$$\int_0^{t_0} (\sigma - \Delta\sigma)^n dt = \int_0^{t_0} \sigma^n dt - E(\epsilon_p, t_0) \qquad (1.5.4)$$

where it is assumed that strain hardening depends upon plastic strain. Further,

$$\int_0^{t_0} \sigma^n dt = \sigma_m^n\, t_0 \int_0^1 [f(\phi)]^n\, d\phi \qquad (1.5.5)$$

where,

$$\phi = \frac{t}{t_0}$$

$\sigma = \sigma_m f(t)$

σ_m = peak stress.

Introducing a new function, which he calls "Form Function" (since it depends upon the form or the shape of the stress),

$$K(n) = \int_0^1 [f(\phi)]^n \, d\phi \tag{1.5.6}$$

we get,

$$H(\epsilon_p) = \sigma_m^n \, t_0 \, K(n) - E(\epsilon_p, t_0) \tag{1.5.7}$$

By combining the last term with Flow Function we get,

$$\sigma_m^n \, t_0 \, K(n) = G(\epsilon_p, t_0) \tag{1.5.8}$$

where,

$$G(\epsilon_p, t) = H(\epsilon_p) + E(\epsilon_p, t_0) \tag{1.5.9}$$

= Flow Function corrected for strain hardening.

The "Flow Function" and "n" can be determined experimentally and then the above equation can be used to predict the amount of plastic strain corresponding to any known stress function.

1.6 Application of the Design Equation

Let us assume that a material is subjected to a stress which appears as shown in Figure 7. Dividing the ordinates by the peak stress and the abscissas by the duration of loading we get a dimensionless function as shown in Figure 8.

Knowing "n", we can find out the value of the Form Function for the present loading. Thus the terms on the left hand side of equation (1.5.7) are known and, therefore, the product can be evaluated. This should be equal to the corresponding Flow Function. The corresponding plastic strain can then be determined using the Flow Function curve as illustrated in Figure 9. This will be equal to ε_1 or ε_2 or ε_3 depending upon the duration of loading. In between results may be obtained by interpolation.

Thus, with only two material parameters, the Design Equation relates the plastic strain to the applied stress.

1.7 Determination of the Material Parameters

For small strains, the strain hardening is almost negligible. Equating two cases of almost equal strain and assuming the Form Functions to be almost equal (which is true for small strains) we get,

$$\sigma_{m_1}^{\ n}\, t_1 \simeq \sigma_{m_2}^{\ n}\, t_2 \qquad (1.7.1)$$

or,

$$n = \frac{\ln(t_2/t_1)}{\ln(\sigma_{m_1}/\sigma_{m_2})} \qquad (1.7.2)$$

Once "n" is known, Form Functions can be calculated using equation (1.5.6) and equation (1.5.8) can then be used to calculate Flow Function.

The main problem is, therefore, to carefully select two cases of small and equal plastic strain.

CHAPTER 2

TEST PROCEDURES

2.1 Description of the Test Equipment

The considerations and details of the design of the test equipment have been given in Appendix I. A brief description is given below.

Figure 1 shows a general view of the complete set up. It consists mainly of a Drop Table and a Hydraulic Intensifier. Other important accessories include a Release Mechanism for releasing the table and a Latching Mechanism for holding the table after its first bounce.

The intensifier consisting of a Drive Piston of small diameter, a Loading Piston of large diameter and an Oil Chamber connecting the two is shown in sectional view in Figure 6. It was obtained from McGill University and was used without modification.

Figure 6 also illustrates the mounting of the sample. The sample sits on the bottom anvil which is mounted on the top of a Baldwin Lima Hamilton, Type C, 50000 lbs. strain gauge load cell. On the top of the sample is the top anvil, the loading piston rests on the latter.

The blow given to the drive piston by the table, as it falls, is multiplied by the intensifier. As a result, the loading piston applies a steady compressive force to the sample. This force is

transferred to the load cell which generates a signal proportional to the force and the voltage of the battery. A heavy duty, 6 volts, dry cell battery was used for this purpose. The signal was then fed to the differential amplifier, Type 3A3 of Tektronix Oscilloscope, Type 564, having storage type screen. The load pulse was then recorded on the screen with suitable amplification.

The duration of loading was obtained by measuring the base of the load pulse and by knowing the time scale of the trace.

To ensure that the complete load pulse was displayed and, at the same time, to utilise the maximum area of the screen, it was necessary to use a triggering mechanism, which started the sweep at the instant when the table was just about to strike the drive piston. This was done by means of a microswitch mounted on the main frame. In the normal case, the switch remained open. The grid of the oscilloscope was given a negative bias. When the table was about to come in contact with the drive piston, a Striker, mounted on the table, closed the microswitch. The tube was fired and a sweep was stored on the screen. In this way, triggering at the right instant was achieved.

Care had to be taken in adjusting the level of the negative bias in the grid. If it was too great, the voltage from the microswitch would not be sufficient to overcome the bias and, consequently, the tube would not fire. On the other hand, if it was too small, electrical noise in the system might cause false firing.

The methods of mounting and operating the microswitch are shown in Figure 5.

A hydraulic hand pump was used for pumping oil in the oil chamber. A 2000 p.s.i., Model C, Heise Gauge measured the pressure in the chamber. A 1/8 ton electric hoist chain lodestor, mounted at the top of the main frame raised and lowered the drop table. The height of the drop table was indicated by a pointer resting upon a 6 foot scale mounted on the frame. A polaroid camera, attached to the oscilloscope, was used to take the photographs of the load pulse.

2.2 Setting Up The Equipment For a Test

To start, the intensifier was filled with oil (Aero Shell Fluid 4) and all entrapped air in the chamber was carefully bled away through the air vent. The air vent was then closed and the sample was mounted as explained earlier. Oil was then pumped in to generate a bias pressure of 100 p.s.i. in the chamber. This was necessary to avoid backlash in the system. The inlet to the oil chamber was then closed by means of a 6000 p.s.i., 1/4" Needle Stop Valve. The table was raised to a predetermined height by means of the lodestor. Sensitivity of the amplifier and the time scale of the oscilloscope beam were selected and the flourescent screen was set to store the pulse. The aperture and the duration of exposure of the camera were set to necessary values. The latching mechanism, the triggering level and

the circuit of the load cell with the battery were checked. When all these checks had been made, the equipment was ready for a test.

The dimensions of the samples, before and after tests, were measured with the help of No. 656-617 Starrett Dial Indicator having an accuracy of 0.0001" and a range of 0.4". The range was extended by using "Jo" blocks. The permanent strain in the sample was calculated from the permanent set and the initial length.

The weight of the table was determined by suspending the entire assembly from a spring balance. This gave the weight of the falling mass.

2.3 Calibration Of The Test Equipment

Calibration was done for the determination of the peak stresses and the durations of loading for the different combinations of mass and volume and for different heights of drop. Fully hardened samples (of tool steel), having the same dimensions as those of the test samples, were used for this purpose.

The analysis in Appendix I shows that the duration of loading depends upon the mass of the falling table and on the total volume of oil in the oil chamber. Thus, for a particular combination of mass and volume, there will be a definite duration of loading. Some of these results are tabulated in Table 2 of Appendix III.

The peak stresses for different heights of drop were determined for some combinations of "Mass and Volume". The curves obtained from these results represented the characteristics of the test equipment.

According to theoretical analysis, these curves should obey a linear relationship, when plotted on a log-log scale, having a constant slope of 0.5. The intercept of these curves should vary with the variation in "mass-volume" combination. But the actual results are different as can be seen in Figure 21. This may be due to internal friction - in the intensifier, loss of momentum of the table due to guided fall,or presence of some entrapped air inside the oil chamber.

Three basic drop tables of different weight values were used. Further weight variations were obtained by attaching additional masses - the lightest table weighed 18 lbs.

The volume of the oil chamber was changed by inserting spacers within the chamber. The minimum volume, using the largest spacer, was 8 cubic inches.

2.4 Sample Preparation

Armco Ingot Iron was used as the test material. It was procured from Corey Steel Co., Chicago, Illinois. The main aim of the present work was not to determine the properties of any specific material, but to design a test equipment for determining these properties. Armco Ingot Iron was tested because this material was also being investigated by the Metallurgical Engineering Department of McMaster University for impact strength.

Armco Ingot Iron is 99.8% pure iron. Chemical analysis indicated the presence of the following impurities:

C	= 0.022% ;	Mn	= 0.028% ;	P	= 0.005%
S	= 0.018% ;	Si	= 0.003% ;	Cu	= 0.052%

The material was obtained in the form of cold worked rods, about half an inch in diameter and approximately thirty inches long. It was machined and cut into medium size cylindrical samples with tolerances as prescribed by ASTM standard E9-61T [12]. After machining, the samples were fully annealled.

Annealing was done in the Metallurgical Engineering Department of McMaster University. There were about sixty samples. As the furnace could only accommodate twenty-nine samples at a time, the samples were divided into two batches and annealled to different durations to allow the effects of softness to be studied. An atmosphere of pure Argon was used to prevent oxidation.

The two batches were treated as follows:

Batch	Temperature of Annealing	Duration
A	925°C	30 minutes
B	925°C	60 minutes

Both batches were allowed to cool to room temperature inside the furnace.

After annealing, the samples were polished by dipping them into dilute hydrochloric acid.

A three-digit identification number was given to all the samples. The first digit represented the batch, the second, the duration of loading, and the third, the serial number of the sample in a particular

test. When more than nine samples were tested in any particular test, the number of digits was increased to four. In that case, the last two digits represented the serial number of the sample in that particular test.

The photographs of the stress-pulse were given the same number as that of the corresponding sample.

2.5 The Static Test

The material was tested for the amount of permanent strain corresponding to a known stress in static condition. Each sample was loaded only once. The results were to be compared with those of dynamic tests. Moreover, this information was needed for estimating the range of the dynamic tests.

The hydraulic intensifier was used for static tests. A sample was mounted on the load cell and pressure was created in the oil chamber to a certain limit. The actual pressure was recorded by means of the Heise Gauge. The static stress was calculated from a knowledge of the areas of the loading piston and the sample. The pressure was maintained constant for some time and then it was released. The permanent strain in the sample was calculated from the amount of the permanent set and initial length of the sample.

2.6 The Dynamic Test Plan

It was decided to limit the range of investigation within 5% plastic strain since, in practice, one is generally not interested in very large strains. The force required to produce this strain

for the first test, was estimated from the results of the static tests. The range was then subdivided to give an even distribution of the test points. Subsequent tests were based upon the information available from the previous tests.

CHAPTER 3

TEST RESULTS

3.1 Some Typical Traces

Some Typical traces of the stress-pulse are shown in Figures 29 to 36.

Figure 29 shows a stress-pulse corresponding to a fully hardened sample. There is absolutely no yield and, therefore, this represents the characteristic pulse generated by the present equipment. As expected, the shape is sinusoidal.

Figure 30 was obtained by superimposing two traces for the same combination of mass and volume but for different heights of drop. This figure illustrates that the duration of loading is independent of the height of drop. Peak stress increases with the increase in the height. Therefore, the peak stress can be changed without changing the duration of loading.

Figure 31 is a trace showing very little yield by the material. The pulse transmitted is still approximately sinusoidal.

Figure 32 shows some yield by the material. It is to be noted here that the rising portion of the pulse is nearly sinusoidal while the decreasing portion is close to triangular. It indicates that the actual duration of loading increases with the yielding of the material. This deviation, however, is small.

In Figures 33 to 36, the actual peak stress is much less than the nominal peak stress expected for the particular combination of mass, volume and height, showing a large amount of yield. At the same time, the duration of loading is more than the nominal duration.

3.2 Static Test Results

The results of the static tests are given in Table 3 of Appendix III.

Curves of plastic strain versus applied stress were plotted for the two batches. This is shown in Figure 22. They show that for any applied stress the total plastic strain in Batch B is more than that in Batch A. It is evident that Batch B is softer than Batch A. This was expected because Batch B was annealled for a longer period and, therefore, had more time for grain-growth.

The dimensions of the samples, before and after static tests, are given in Table 7 of Appendix III.

Table 6 gives the necessary information for the above calculations.

3.3 Dynamic Test Results

The results of the dynamic tests are given in Table 4 of Appendix III.

The peak stress-plastic strain curves of dynamic tests were plotted and superimposed on the similar curve of the static test. These are shown in Figures 23 and 24 for the two batches. All these curves were then plotted on one graph as shown in Figure 37 for comparison purposes. The average values of the Stress Dislocation Velocity Exponent "n", were found as given below:

n = 5 for Batch A

n = 6 for Batch B

Form Functions and Flow Functions were then calculated on the basis of these values. The latter were plotted against plastic strain as shown in Figures 25 and 26.

The test results corresponding to large plastic strains revealed that the actual peak stress was much less than the nominal peak stress (as obtained from the characteristics of the equipment for the particular combination of mass, volume and height). This was because the resistance offered by the material was much less than the applied stress. To study the yielding phenomenon in the dynamic case, the corresponding nominal stresses were calculated and plotted against plastic strain. These are shown in Figures 27 and 28. It is interesting to note that when plotted on semi-log paper they follow a linear relationship. When extended, these lines converge to a point near zero plastic strain. The peak stress, corresponding to zero plastic strain, may be considered as the dynamic yield stress of the material. In the present investigation, this stress was found as follows:

Dynamic Yield Stress

18,000 p.s.i. for Batch A

17,000 p.s.i. for Batch B

The dimensions of the samples, before and after the dynamic tests, are given in Table 8 of Appendix III.

3.4 Conclusions

It was noted that the values of "n" were very low when compared with similar values of other materials. The reason for this may be that, compared with the other materials investigated earlier, Armco Ingot Iron is very soft.

The curves of plastic strain versus applied stress show that the present material is very sensitive to strain rates. In the static case, the material shows a plastic strain of about half percent under a stress of 15,000 p.s.i. Whereas, in the dynamic case, it shows absolutely no plastic strain under a stress approximately twice as high. It indicates that, though the static yield stress of the material is below 15,000 p.s.i., it can be safely loaded to a stress of 25,000 p.s.i., if the load is applied for only a short duration (40 milliseconds or less).

It is to be noted further, that Batch B is more sensitive to strain rate than Batch A. This illustrates that softer material is more sensitive. This agrees with the theory of high strain rates.

The plots of Flow Function versus plastic strain show a lot of scatter. There can be various reasons for the same. First, it was very difficult to maintain a constant duration of loading as the material tested was very soft. Second, the number of samples

was very limited and it was difficult to draw good inference from just a few points. Third, the method used in the measurement of the voltage of the battery was crude.

CHAPTER 4

RECOMMENDATIONS FOR FUTURE WORK

In the course of testing, some limitations in the present equipment were experienced. It is recommended that for future work, the following amendments be made;

(i) For the present work Aero Shell Fluid 4 (having a low Bulk Modulus) was used - a better oil was not available in the local market. As the duration of loading depends upon the Bulk Modulus of the oil, this should be replaced by some other oil having high Bulk Modulus.

(ii) The signal generated by the load cell is proportional to the voltage of the battery. Any error encountered in the measurement of this voltage greatly affects the results. Therefore, this reading must be very accurate. A millivoltmeter should be used for this purpose.

(iii) For a comparison on the signal generated by the load cell, it is better to measure the peak pressure in the oil chamber by using a pressure transducer.

(iv) The present spacers should be modified to fill the inside space of the oil chamber completely and reduce the final volume of the chamber. This will help in reducing the duration of loading.

CHAPTER 5

REFERENCES

1. Hopkinson, B., "on the Rupture of Iron Wire by a Blow", Proceedings of the Royal Society A74 (1905), 498.

2. Davis, E. A., "The Effect of the Speed of Stretching and the Rate of Loading on the Yielding of Mild Steel", Journal of Applied Mechanics, Dec. 1938, A137.

3. Manjoine, M. J., "The Influence of Rates of Strain and Temperature On Yield Stresses of Mild Steel", Trans. A.S.M.E., Vol. 66, 1944.

4. Clark and Wood, "Time Delay for the Initiation of Plastic Deformation of Rapidly Applied Constant Stress", Proc. A.S.T.M., Vol. 49, 1949.

5. Clark, D. S. "Behaviour of Materials Under Dynamic Loadings", Trans. A.S.M., Vol. 46, 1954.

6. Dieter, G. E., Mechanical Metallurgy, McGraw-Hill Book Co. Inc.

7. Campbell, J. D., "Dynamic Yielding of Mild Steel", Acta Metallurgica, Vol. 1, 1963.

8. Yokobori, T., "The Cottrell-Bilby Theory of Yielding of Iron", Physical Review, Vol. 88, 1952, 1423.

9. Hahn, G. T., "A Model for Yielding with Special Reference to The Yield Point Phenomenon of Iron and Related B.C.C. Metals", Acta Metallurgica, Vol. 10, Aug. 1962.

10. Gilman, W. G.& W. G. Johnston, "Dislocation Velocities, Dislocation Densities and Plastic Flow in Different Crystals", Journal of Applied Physics, Vol. 20, 1959.

11. Kardos, G., "A Study of Plastic Flow in Steel at High Rates of Strain", Ph.D. thesis, Department of Mechanical Engineering, McGill University, Montreal, Quebec, 1965.

12. A.S.T.M. "Tentative Method of Compression Testing of Metallic Materials", A.S.T.M. E-61T.

APPENDIX I

DESIGN OF THE TEST EQUIPMENT

DESIGN OF THE TEST EQUIPMENT

I.1 Basic Aim

The main requirements of the present equipment may be briefly stated as follows:

(i) Generation of a single blow on the material.

(ii) The stress function to be independent of the response of the material (to get identical pulse shapes for at least two cases of small plastic strain).

(iii) A means of varying the peak stress without changing the duration of loading (to get curves of Flow Function for constant durations).

A falling mass and a spring was considered as the basic concept for the design. Analysis shows that this design can satisfy all the above mentioned conditions.

I.2 Analysis of the System

Figure 10 illustrates a simple "Spring - Mass" system with necessary details.

We can write the initial conditions as,

$$x = 0 \qquad \text{at} \qquad t = 0$$

$$v = \sqrt{2gh} \qquad \text{at} \qquad t = 0$$

The displacement of the spring will be given by,

$$x = \sqrt{\frac{2ghm}{k}} \; \text{Sin} \sqrt{\frac{k}{m}}\, t \qquad \text{(I.2.1)}$$

The force in the spring will be,

$$F = m\ddot{x} = -\sqrt{2ghmk}\ \sin\sqrt{\frac{k}{m}}\,t \qquad \text{(I.2.2)}$$

And the period of oscillation T will be,

$$T = \frac{2\pi}{\sqrt{k/m}} = 2\pi\sqrt{\frac{m}{k}} \qquad \text{(I.2.3)}$$

Hence, the peak force experienced by the spring,

$$F_{max} = -\sqrt{2ghmk} \qquad \text{(I.2.4)}$$

The negative sign indicates that the force is compressive.

The duration of loading will be equal to half of the period of oscillation.

Hence, duration of loading, $t_o = \pi\sqrt{\frac{m}{k}}$ (I.2.5)

Equation (I.2.5) shows that the duration of loading is independent of the height of drop. Whereas, equation (I.2.4) shows that the peak force varies with the height of drop. Thus the peak force can be changed by changing the height of drop whilst maintaining constant duration. The stress function will be sinusoidal and will depend on the parameters of the system and, therefore, will be independent of the response of the material.

I.3 Physical Form

A hydraulic intensifier, as illustrated in Figure 12, was selected to serve as the spring. Pressure in the oil chamber is equivalent to the stiffness of the spring. The falling mass gives a blow to the drive piston. Pressure is created in the chamber and load is transmitted to the specimen through the loading piston. The mass jumps back due to "Spring Action" and the load is released.

It is to be noted that the duration as well as the peak force depends upon the stiffness of the spring. Therefore, we must find out the factors controlling the equivalent stiffness of the present system. This can be done as follows:

The reduction in volume, dV (neglecting the small volume swept by the loading piston) due to a force F on the drive piston will be given by,

$$dV = A\, dx \tag{I.3.1}$$

where,

V = Volume of oil,

A = Area of the drive piston, and

dx = The distance moved by the drive piston

But the volumetric strain is given by,

$$\epsilon_v = \frac{dV}{V} = \frac{p}{K'} \tag{I.3.2}$$

where,

p = Pressure in the chamber,

K' = Bulk modulus of elasticity of oil,

and stiffness is defined as the force necessary for unit displacement. Thus,

$$k = \frac{F}{dx} \tag{I.3.3}$$

From equations (I.3.1), (I.3.2) and (I.3.3) we get,

$$k = \frac{K'A}{V} \tag{I.3.4}$$

Substituting equation (I.3.4) in equations (I.2.4) and (I.2.5) and remembering that K',A and g are constants, we find that,

$$t_o \propto \sqrt{mV} \tag{I.3.5}$$

and

$$F_{max} \propto \sqrt{\frac{mh}{V}} \tag{I.3.6}$$

I.4 Other Requirements

The requirements for generating a single blow means that there should be some device to hold the mass after its first bounce. A "Latching Mechanism" was designed for this purpose. The detailed design of this mechanism is given in Section 1.5.3.

Another requirement is to have a device to release the mass from different heights. This appears to be very simple but

complications arise when heavy weights have to be released. For the device to be positive, the weight must hold up under its own weight and at the same time it must fall whenever desired. A "Release Mechanism" was designed for this purpose. The detailed design of this mechanism is given in Section I.5.2.

I.5 Detail Design

1.5.1 Design of the Main Frame

For natural performance, controlled horizontal movement but free fall of the falling Mass (from now onwards, the falling mass will be termed as the table) was desired. To meet this requirement the main frame was constructed from angle section. The second consideration was the lateral force which is developed at the time of holding the table immediately after its first bounce. The whole inertia force has to be resisted by the frame. In order to reduce the lateral deflection during this time, the cross-section of the frame was further increased by providing stiffeners as shown in Figure 14. For further rigidity, the two angle-sections were fastened at a height of about seven feet from the ground by means of a pair of stiffening rods, as can be seen in Figure 1.

At the top of the frame, provision was made to mount a 1/8 ton lodestor (electric chain hoist) which was used for lifting the table. An angle flange was welded to the bottom of the frame flush with the adjacent forces of the base of the intensifier as shown schematically in Figure 13.

I.5.2 Design of The Release Mechanism

A critical element of the design was the release mechanism. Its reliable functioning was essential to the efficient performance of the experiment. The following points were considered necessary for obtaining this reliability:

(i) The weight of the table should keep the mechanism in locked position.

(ii) The release of the table, by some external means, should be assisted by the weight of the table.

(iii) The force needed to operate the external device should be small.

(iv) The switching from "Locking Under its Own Weight" to "Release Under its Own Weight" should be positive.

The mechanism designed to satisfy these requirements is shown in full detail in Figure 4. Its working has been explained, schematically, through Figures 15 and 16.

Figure 15 illustrates the locked position. Due to the weight W of the table, a moment M is produced in the main links. This creates a force F in the small links. As a result a force P is exerted on the central block acting in the upward direction because of the geometry. The central block is prevented from moving upwards by the stopper (No. 6).

The main links can be separated only when the central block is made to move downwards. Force P is opposing this movement and therefore is acting as a locking force generated by the weight of

the table. The heavier the table, the greater is force P and, therefore, the stronger is the locking.

When there is no load, the central block is pulled up by the springs (No. 1).

When the solenoid (No. 2) is energized, it pulls the central block against the force P. When the central block passes over the dead centre position, the direction of the force P changes due to the change in the geometry. The new position is shown in Figure 16. This force now adds to the pull of the solenoid. In this way, the weight of the table helps in the releasing operation. The mechanism, therefore, is reliable in both the cases,

As force P is small, the third condition is automatically satisfied. Force P can be further reduced, if desired, by making a small change in the geometry of the mechanism. The relasing operation has been illustrated in Figure 17.

It should be noted that the force P is proportional to "e" (the amount of deviation of the central block from the dead centre position). If "e" is too large, the solenoid cannot pull the central block. On the other hand, if "e" is too small, there is a possibility that some small fluctuations may cause the central block to pass over the dead centre position. In the present mechanism, these troubles were avoided by means of an adjustable stopper.

I.5.3 Design of the Latching Mechanism

The latching mechanism is required for the immediate removal of the load after the first bounce. The reliability of the whole equipment is dependent upon the reliable operation of this mechanism. The overall requirement may be summarized as the following:

(i) It should not obstruct the motion of the table during the initial fall.

(ii) The table should be free to move upwards during the bounce to allow the immediate removal of the load.

(iii) It should not allow any downward motion of the table after the first bounce.

(iv) The mechanism should work for all heights of drop (including very small drops).

Analysing the above requirements, we find that the desired motions of the table are as follows:

Case	Direction	Condition
First Fall	Upward	Free
	Downward	Free
Second Fall	Upward	Free
	Downward	Not Allowed

It is evident that some mechanism has to be introduced between the first and the second falls.

A cam type latch, mounted on the table, was selected for this purpose. Figure 18 shows this latch in two positions.

Position A is the Off position of the latch. There is a gap "d" between the latch and the inner edge of the angle-section. In this configuration, the latch, and the table, are free to move both upwards and downwards.

Position B is the "Locked" position. Point B is in contact with the inner edge of the angle and any motion of the latch will be accompanied with rolling. If the latch is moved upwards, rolling will cause point B to move down and some other point E will occupy the position of the point B. Since OE is less than OB, the latch will not roll but will slide on the edge. Thus upward motion of the latch, and therefore of the table, is allowed. But when the latch is moved down, rolling will require point B to move up and some other point C will tend to occupy the position of point B. But since OC is greater than OB, this will not be possible unless the gap is increased.

With this mounting, if the latch is maintained in position A during the first fall and in position B during the second fall, the table will have conditional motions as desired above.

The problem now is to change the configuration of the latch from position A to position B after the first fall and before the second fall.

The basic scheme is explained in Figure 19. As is seen, a hook (No. 5), suspended from the table (No. 1), holds the latch through a Rod (No.6). A striker (No.7), attached to the other end of the hook, moves up and down with the table. If the striker is pushed up, the hook will try to swing around the fulcrum in the clockwise direction. But this is prevented by the rod. On the other hand, if the striker is pushed down, the hook will swing in the anti-clockwise direction as there is no obstruction. The rod will be released from the hook and the support of the latch will fall. The latch will, then, swing under its own weight and will orient itself in position B. A tension spring (No.3) is mounted between the table and the latch to create extra force in order to facilitate quick change from position A to position B.

A device was made to make the above change during the fall of the table. This is shown in Figure 20.

A lever (No.2) is hinged at one end and is supported by a light spring (No.3) at the other end. It can swing to a certain limit in the lower direction but is prevented from swinging in the upper direction by the stopper (No.4). As the table falls, the striker pushes the lever down. An upward force is experienced by the striker but it does not make any change in the mechanism for reasons explained above. When the table moves up, the upward movement of the lever when pushed by the striker is prevented by the stopper. The downwards force on the striker causes the hook to swing. The latch

is released and immediately orients itself into position B.

The overhang LC of the lever needs some important considerations. It is to be noted that for release of the latch to occur, the striker must hit the lever from below. It means that it should clear the Lever while it is moving downwards.

Figure 20 illustrates the path of the striker and of the tip of the lever. For a clear pass-over, the minimum height of fall, from the position of the lever, should be equal to "H". Also for the striker to hit the lever on the striker's jump, the minimum height of jump must equal "H". But the height of jump is proportional to the height of drop. Therefore, for the mechanism to be effective on very small drops it is necessary that "H" should be very small. The illustration shows that "H" can be reduced to "H'" by reducing the overhang LC to LC'. But at the same time, the overhang cannot be reduced very much because provisions must be made for the inherent plays present in every system.

Figures 2 and 3 show the details of this mechanism as used in the present equipment.

APPENDIX II

SAMPLE CALCULATIONS

SAMPLE CALCULATIONS

II.1 General Calculation

A typical "Record Sheet" is illustrated on page 42. All information was entered in the respective position.

The signal generated by the load cell had the following rating.

2mV for 50,000 lbs. per volt of battery input

During a particular test (sample No. 113), the battery showed a voltage of 5.85 volts. Hence the rating of the load cell was,

$$2 \times 5.85 \text{ mV for } 50{,}000 \text{ lbs.}$$

or

$$1 \text{ mV for } 4{,}273 \text{ lbs.}$$

Therefore, Peak Force = Sensitivity x Scale Reading x 4273 lbs./mV.

$$= \frac{0.2 \text{ mV}}{\text{cm}} \times 4.78 \text{ cms.} \times \frac{4273 \text{ lbs.}}{\text{mV}}$$

$$= 4084.99 \text{ lbs.}$$

This force was corrected for the bias pressure.

Actual Peak Force = Apparent Peak Force + Force due to bias pressure

$$= 4084.99 + 100 \times 8.2957$$

$$= 4914.56$$

Therefore Peak Stress = $\frac{\text{Peak Force}}{\text{Area of the Specimen}}$

DYNAMIC LOAD TESTS RECORD SHEET

Date: October 11th, 1967

Weight of Table:	23 lbs.	Cylinder Volume:	8 cubic inches
Zero Reading of Scale:	2"	Battery Voltage:	5.85 volts
Initial Height:	7"	1 Millivolt ≡	4273 lbs.
Height of Drop:	5"	Batch No.	A
Oscilloscope		Sample No.:	113
Sensitivity:	0.2 mV/cm.	Final Height:	4"
Time Base:	5 ms./cm.	Height of Jump:	2"
Peak Ordinate of Pulse:	4.78 cm.	Peak Force:	4914.5 lbs.
Base of Pulse:	3.48 cm.	Time of Loading:	17.4 milliseconds
Photograph No.:	113		

Bias Pressure Checked:	Yes
Oscilloscope Settings Checked	Yes
Camera Checked	Yes
Latching Mechanism Checked	Yes
Triggering Level Checked	Yes
Sample Mounting Checked	Yes

Dimensions of Samples (in inches)

	Diameter	Length
Initial:	0.4428	1.3505
Final:	0.4432	1.3493
Reduction in Length:		0.0012
% Plastic Strain:		0.088

$$= \frac{4914.56}{\frac{n}{4} \times (0.4428)^2} \text{ p.s.i.}$$

= 31892 p.s.i.

Calculation of plastic strain is illustrated on the "Record Sheet".

II.2 Determination of "n"

For very small plastic strain, the load pulse may be considered to be sinusoidal. Equating the Flow Functions for equal plastic strains, the value of "n" can be determined.

BATCH A

SERIAL	PEAK STRESS (p.s.i)	TIME (ms)	% PLASTIC STRAIN
117	38859	17.4	0.230
123	33925	34.2	0.244

Using the Characteristic Equation we get,

$(38859)^n \times 17.4 \times K(n) = H(0.230)$ and

$(33925)^n \times 34.2 \times K(n) = H(0.244)$

Assuming H(0.230) to be approximately equal to H(0.244) and neglecting any difference in Form Functions we get,

$(38859)^n \times 17.4 = (33925)^n \times 34.2$

By solving this equation we get,

n = 4.88

BATCH B

SERIAL	PEAK STRESS (p.s.i.)	TIME (ms.)	% PLASTIC STRAIN
211	39594	18.6	0.044
231	30111	42.0	0.044

As before,

$$(34594)^n \times 18.6 \times K(n) = H(0.044) \quad \text{and}$$

$$(30111)^n \times 42.0 \times K(n) = H(0.044)$$

Equating the two we get,

$$(34594)^n \times 18.6 = (30111)^n \times 42.0$$

Solving which we get,

$$n = 5.86$$

II.3 Evaluation of Form Function

Form Functions were evaluated by the method of Numerical Integration using Simpson's Repeated Rule. The area of the stress-pulse was divided into twenty equal parts. Ordinates at the above interval were measured by projecting the photograph of the pulse on the screen of Nikon Profile Projector, Model V-16, with a magnification of ten. Measurements were taken with the two micrometers mounted on the table of the Projector. The range of these micrometers was extended by using standard "Jo" Blocks.

The detail procedure is given on pages 45 and 46.

EVALUATION OF FORM FUNCTION

Photograph No. 113 n = 5

1 cm. of photograph length is equivalent to 0.369" of table movement.

Calculation of Base Length:

Reading at the Initial Point: 1.280"

Reading at the Final Point: 0.000"

Base Length = 1.280"

$$\text{Interval} = \frac{\text{Base Length}}{20} = 0.064"$$

Peak Ordinate = 1.775"

POINT NO.	ABSCISSA (inches)	ORDINATE (inches)	ORDINATE AS A FRACTION OF PEAK ORDINATE (Y)	$(Y)^n = Z$
1	0.000	0.000	0.00000	0.00000
2	0.064	0.771	0.43437	0.01546
3	0.128	0.808	0.45521	0.01955
4	0.192	0.985	0.55493	0.05262
5	0.256	1.225	0.69014	0.15656
6	0.320	1.385	0.78028	0.28924
7	0.384	1.531	0.86253	0.47739
8	0.448	1.650	0.92957	0.69408
9	0.512	1.738	0.97915	0.90000
10	0.576	1.772	0.99831	0.99158
11	0.640	1.763	0.99324	0.96665
12	0.704	1.713	0.93507	0.71486
13	0.768	1.611	0.90760	0.61585
14	0.832	1.488	0.83831	0.41402
15	0.896	1.325	0.74648	0.23179

16	0.960	1.142	0.64348	0.11032
17	1.024	0.926	0.52169	0.03864
18	1.088	0.691	0.38929	0.00894
19	1.152	0.482	0.27155	0.00148
20	1.216	0.271	0.15268	0.00015
21	1.280	0.000	0.00000	0.00000

The Form Function is therefore equal to,

$$\frac{1}{3} \times \frac{1}{20} \left[(z_1 + z_{21}) + 4 \sum_{i=1}^{10} z_{2i} + 2 \sum_{i=1}^{9} z_{2i+1} \right]$$

$$= \frac{1}{60} [0.00000 + 5.15252 + 3.40791]$$

$$= 0.28534$$

II.4 Evaluation of Flow Function

Once the Form Function was known, it was very easy to calculate Flow Function using equation (1.5.8). An illustration, for the above mentioned sample is given below.

Sample No.:	113
Peak Stress:	31892 p.s.i.
Duration of Loading:	17.4 milliseconds
Form Function:	0.28534
Plastic Strain:	0.088%

Hence,

$$(\sigma_m)^n = 329.92 \times 10^{20}$$

and

$$H(0.088) = 0.28534 \times 329.92 \times 10^{20} \times 1.74 \times 10^{-2}$$

$$= 163.802 \times 10^{18}$$

APPENDIX III

TABLES

TABLE 1

DELAY TIME

Ratio of Applied Stress To Lower Yield Stress	Corresponding Delay Time
1.1	400 seconds
1.2	6.25 seconds
1.3	548 milliseconds
1.4	97.6 milliseconds
1.5	25.6 milliseconds

TABLE 2

DURATION OF LOADING AS A FUNCTION OF MASS AND VOLUME

Weight of Table	Volume of Oil In The Chamber (cubic inches)	Duration of Loading (milliseconds)
23.0	8	19
35.0	10	22
23.0	112	26
62.5	15	31
41.0	112	35
62.5	112	41

TABLE 3

STATIC TEST RESULTS

BATCH A

Serial	Pressure (p.s.i)	Force (lbs.)	Stress (p.s.i)	% Plastic Strain
1	300	2489	15372	0.325
2	390	3235	19222	0.850
3	500	4148	25604	1.667
4	800	6637	40967	5.000
5	1500	12444	76341	27.70

BATCH B

6	300	2489	15381	0.481
7	420	3484	21480	1.770
8	650	5392	33266	4.900
9	800	6637	41173	7.000

MILLS MEMORIAL LIBRARY
McMASTER UNIVERSITY

TABLE 4

DYNAMIC TEST RESULTS

Serial	Peak Force (lbs.)	Peak Stress (p.s.i)	Time (ms.)	% Plastic Strain
111	3777.9	23306	17.3	0.044
112	4185.5	25804	18.0	0.170
113	4914.5	31892	17.4	0.088
114	5355.0	33137	18.2	0.1185
115	5700.8	34803	17.4	0.2518
116	5880.4	36434	18.6	0.074
117	6299.0	38859	17.4	0.2296
118	6473.6	39887	18.8	0.550
119	6592.3	40543	18.8	0.577
1110	6973.6	42783	19.2	0.800
1111	7143.1	44903	21.8	3.370
1112	7270.3	44521	19.8	1.800
121	3414.3	22762	32.7	0.080
122	4718.0	28963	34.7	0.067
123	5473.6	33725	34.2	0.244
124	5575.3	34437	——*	0.170
125	5735.0	35292	——*	0.1407
126	5743.5	35454	34.7	0.3037
127	5787.2	35701	32.6	0.615
128	6151.6	38020	33.0	0.733
129	6295.7	39422	34.4	1.750
1210	6549.9	40282	32.5	2.150
1211	7143.1	43769	37.2	3.440

Serial	Peak Force	Peak Stress	Time	% Plastic Strain
211	6454.2	36678	18.6	0.044
212	6695.3	40325	18.6	0.288
213	7527.7	42447	18.6	0.548
214	7570.2	44439	——*	0.970
215	7748.8	45515	19.6	1.466
216	4965.8	30634	——*	0.0592
221	5793.5	34073	32.8	0.200
222	6436.4	38280	32.6	0.326
223	6025.7	35328	32.8	0.8592
224	6588.1	38436	33.7	0.585
225	6900.6	40358	33.7	1.140
226	3609.6	21308	——*	0.070
227	7302.4	42946	36.0	2.600
228	7748.8	46849	38.8	4.450
229	7525.6	45616	——*	3.610
231	5695.3	33454	42.0	0.044
232	6007.8	35137	42.6	0.296
233	6025.5	36572	42.4	0.4963
234	6132.8	35868	42.6	0.1926
235	6097.1	35593	42.6	0.963
236	6454.2	38005	42.6	1.415
237	6695.3	39327	43.2	1.911
238	4311.5	25231	39.5	0.022
239	4205.2	26006	38.8	0.030

* The load pulse of this test was partly out of the screen. Therefore, the exact duration of loading could not be noted.

TABLE 5

FORM FUNCTIONS AND FLOW FUNCTIONS

Serial	Time (ms.)	% Plastic Strain	Form Function	Flow Function
111	17.3	0.044	0.35660	42.4193×10^{18}
112	18.0	0.170	0.36489	75.1415×10^{18}
113	17.4	0.088	0.28534	163.802×10^{18}
114	18.2	0.1185	0.33334	242.396×10^{18}
115	17.4	0.2518	0.31542	280.2346×10^{18}
116	18.6	0.074	0.32496	388.005×10^{18}
117	17.4	0.2296	0.32178	491.100×10^{18}
118	18.8	0.550	0.32696	620.600×10^{18}
119	18.8	0.577	0.29997	617.750×10^{18}
1110	19.2	0.800	0.26838	738.600×10^{18}
1111	21.8	3.370	0.35243	1380.525×10^{18}
1112	19.8	1.800	0.22878	792.330×10^{18}
121	32.7	0.080	0.32355	68.642×10^{18}
122	34.7	0.067	0.32942	232.970×10^{18}
123	34.2	0.244	0.24008	368.960×10^{18}
126	34.7	0.3037	0.33390	651.713×10^{18}
127	32.6	0.615	0.33095	625.630×10^{18}
128	33.0	0.733	0.30590	801.960×10^{18}
129	34.4	1.750	0.26858	879.680×10^{18}
1210	32.5	2.150	0.23470	809.000×10^{18}

Serial	Time	% Plastic Strain	Form Function	Flow Function
1211	37.2	3.440	0.25220	1507.030×10^{18}
211	18.6	0.044	0.31997	14.491×10^{24}
212	18.6	0.288	0.29551	23.634×10^{24}
213	18.6	0.548	0.26495	28.825×10^{24}
215	19.6	1.466	0.19860	34.607×10^{24}
221	32.8	0.200	0.31423	24.537×10^{24}
222	32.6	0.326	0.33252	34.108×10^{24}
223	32.8	0.8592	0.26914	17.1612×10^{24}
224	33.7	0.585	0.27626	35.7838×10^{24}
225	33.7	1.140	0.22779	33.1695×10^{24}
227	36.0	2.600	0.20511	46.326×10^{24}
228	38.8	4.450	0.21980	90.170×10^{24}
232	42.0	0.296	0.29377	23.550×10^{24}
233	42.6	0.4063	0.28420	28.832×10^{24}
234	42.4	0.1926	0.30414	27.590×10^{24}
235	42.6	0.963	0.32409	28.070×10^{24}
236	42.6	1.415	0.23110	29.643×10^{24}
237	43.2	1.911	0.24336	38.578×10^{24}
238	39.5	0.022	0.29086	29.640×10^{24}
239	38.8	0.030	0.35915	43.050×10^{24}

TABLE 6

SOME NECESSARY INFORMATION

The Bulk Modulus of the Oil = 18.4×10^4 p.s.i.

The Area of the Drive Piston = 0.8824 sq. inches

The Area of the Loading Piston = 8.29575 sq. inches

The Volume of the Oil Chamber without Spacers = 120.34 cubic inches

TABLE 7

DIMENSIONS OF SAMPLES BEFORE AND AFTER STATIC TESTS

BATCH A

Serial	Initial		Final	
	Diameter (inches)	Length (inches)	Diameter (inches)	Length (inches)
1	0.4541	1.3459	0.4558	1.3415
2	0.4548	1.3501	0.4587	1.3286
3	0.4548	1.3482	0.4577	1.3257
4	0.4577	1.3257	0.4705	1.2583
5	0.4455	1.3502	0.5328	0.9749
	BATCH B			
6	0.4539	1.3402	0.4545	1.3337
7	0.4544	1.3496	0.4592	1.3257
8	0.4539	1.3516	0.4662	1.2855
9	0.4545	1.3337	0.4716	1.2399

TABLE 8

DIMENSIONS OF THE SAMPLES BEFORE AND AFTER DYNAMIC TESTS

Serial	Initial		Final	
	Diameter (inches)	Length (inches)	Diameter (inches)	Length (inches)
111	0.4543	1.3504	0.4544	1.3498
112	0.4544	1.3526	0.4544	1.3503
113	0.4428	1.3505	0.4432	1.3493
114	0.4536	1.3518	0.4536	1.3502
115	0.4569	1.3510	0.4576	1.3476
116	0.4533	1.3513	0.4537	1.3503
117	0.4545	1.3525	0.4563	1.3494
118	0.4545	1.3523	0.4553	1.3479
119	0.4550	1.3485	0.4555	1.3407
1110	0.4556	1.3501	0.4565	1.3393
1111	0.4542	1.3490	0.4628	1.3034
1112	0.4560	1.3495	0.4595	1.3252
121	0.4372	1.3505	0.4372	1.3494
122	0.4553	1.3522	0.4554	1.3513
123	0.4498	1.3494	0.4507	1.3461
124	0.4540	1.3507	0.4545	1.3484
125	0.4549	1.3493	0.4562	1.3474
126	0.4540	1.3510	0.4552	1.3479
127	0.4543	1.3506	0.4558	1.3460
128	0.4539	1.3518	0.4546	1.3419
129	0.4509	1.3503	0.4555	1.3266
1210	0.4550	1.3503	0.4585	1.3512
1211	0.4559	1.3504	0.4639	1.3036

Serial	Initial Diameter (inches)	Initial Length (inches)	Final Diameter (inches)	Final Length (inches)
211	0.4550	1.3501	0.4551	1.3495
212	0.4480	1.3505	0.4486	1.3464
213	0.4541	1.3495	0.4555	1.3421
214	0.4538	1.3505	0.4568	1.3374
215	0.4535	1.3500	0.4574	1.3302
216	0.4543	1.3512	0.4544	1.3504
221	0.4434	1.3509	0.4447	1.3482
222	0.4508	1.3486	0.4527	1.3442
223	0.4541	1.3504	0.4570	1.3388
224	0.4551	1.3473	0.4555	1.3394
225	0.4545	1.3507	0.4575	1.3353
226	0.4525	1.3513	0.4530	1.3504
227	0.4534	1.3523	0.4604	1.3172
228	0.4471	1.3509	0.4580	1.2908
229	0.4466	1.3505	0.4548	1.3017
231	0.4536	1.3490	0.4536	1.3484
232	0.4547	1.3496	0.4558	1.3456
233	0.4462	1.3519	0.4470	1.3452
234	0.4545	1.3487	0.4562	1.3461
235	0.4550	1.3525	0.4554	1.3395
236	0.4531	1.3455	0.4541	1.3264
237	0.4536	1.3515	0.4570	1.3257
238	0.4544	1.3500	0.4544	1.3497
239	0.4539	1.3506	0.4539	1.3502

APPENDIX IV

FIGURES

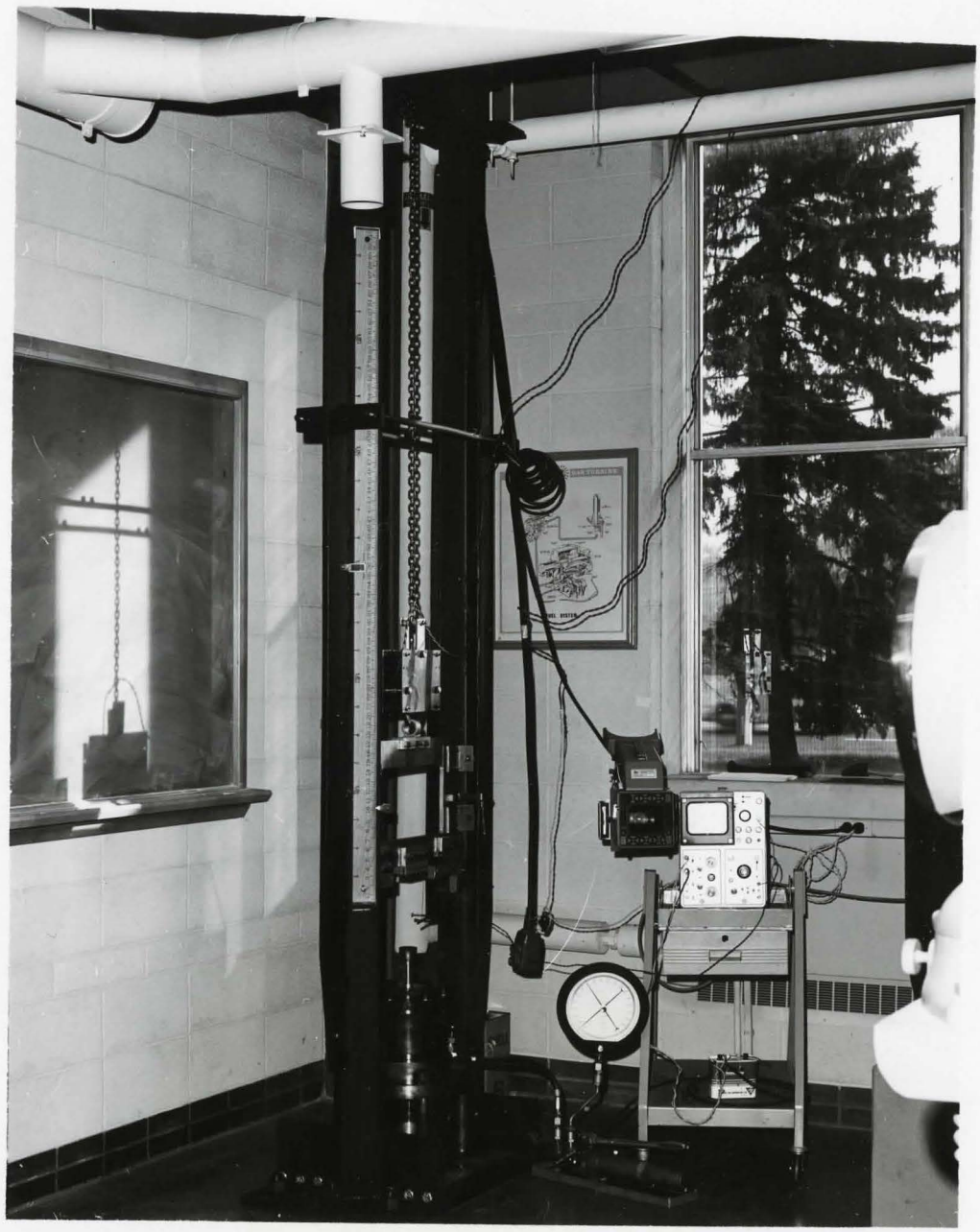

GENERAL VIEW OF THE TEST EQUIPMENT

FIGURE 1

LATCHING MECHANISM IN OFF POSITION

FIGURE 2

LATCHING MECHANISM IN LOCKED POSITION

FIGURE 3

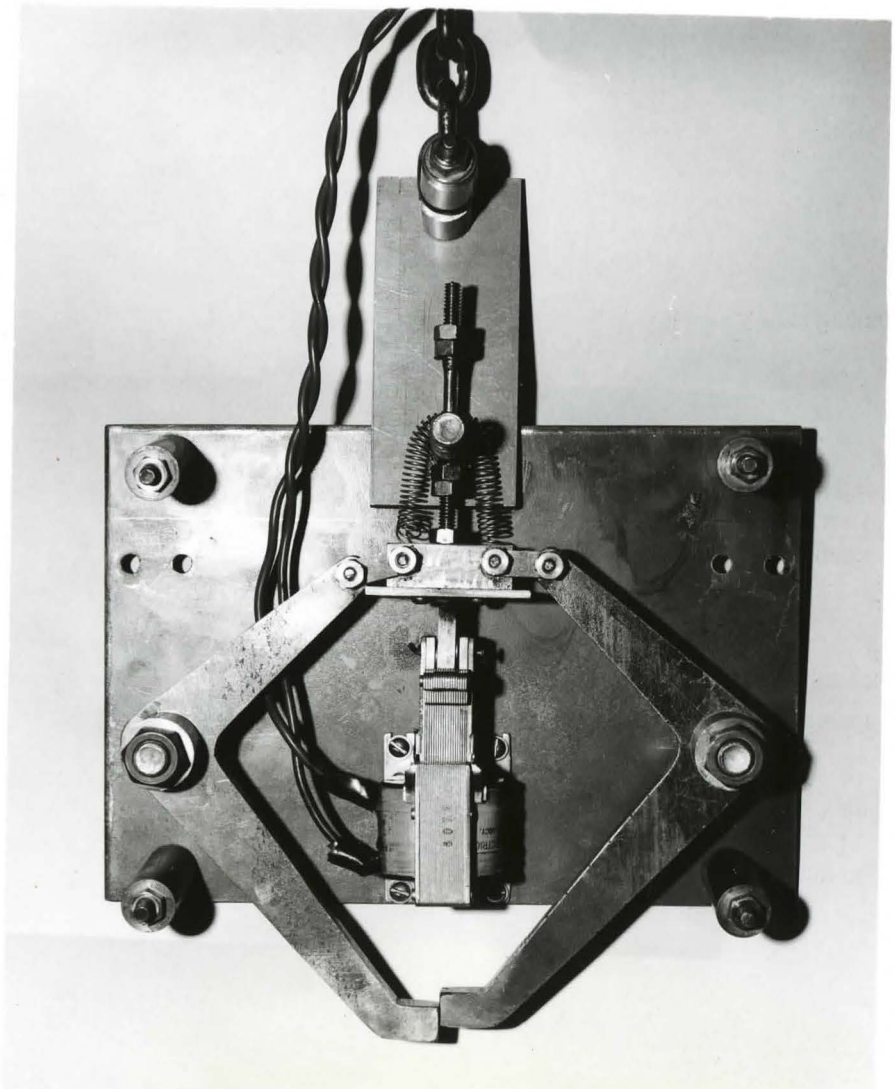

RELEASE MECHANISM

FIGURE 4

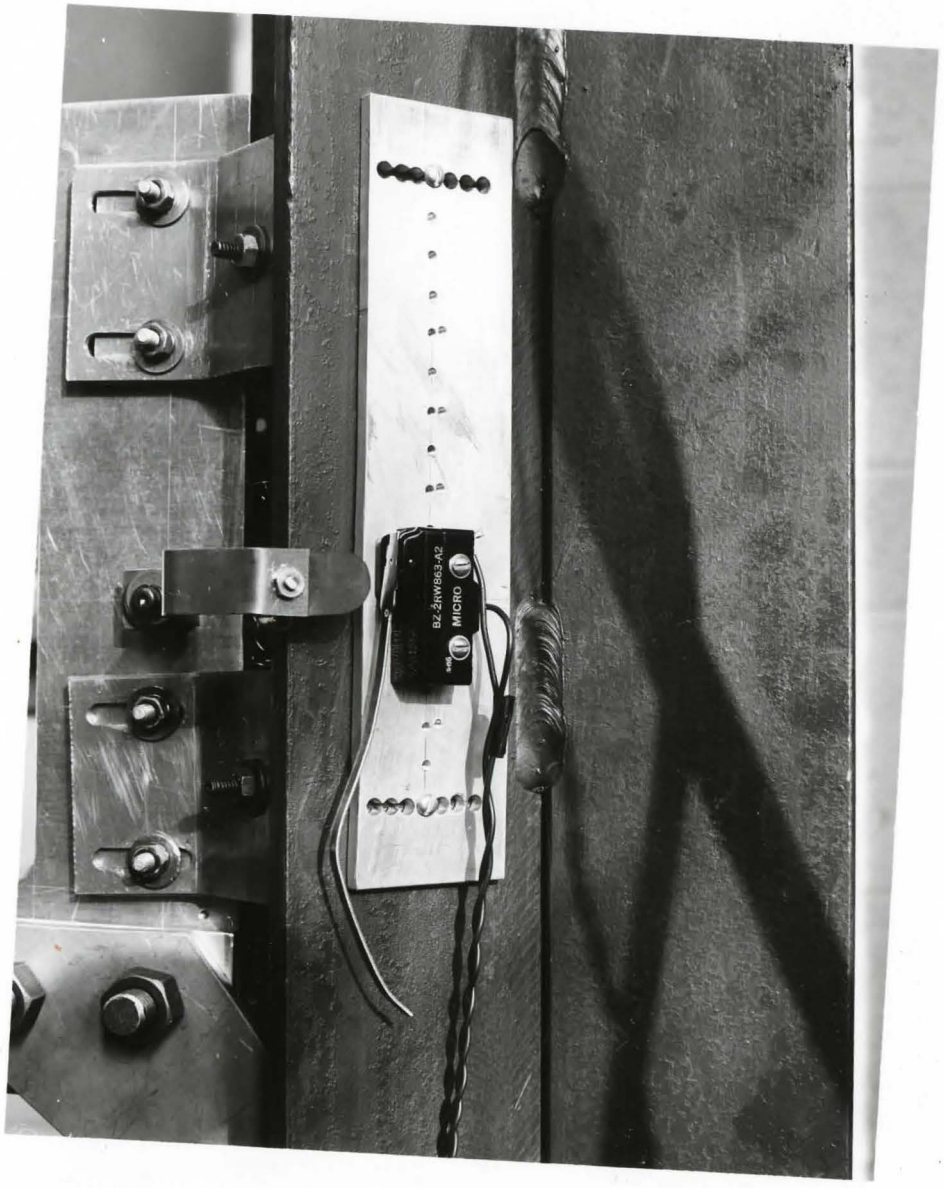

MICROSWITCH AND STRIKER MOUNTINGS

FIGURE 5

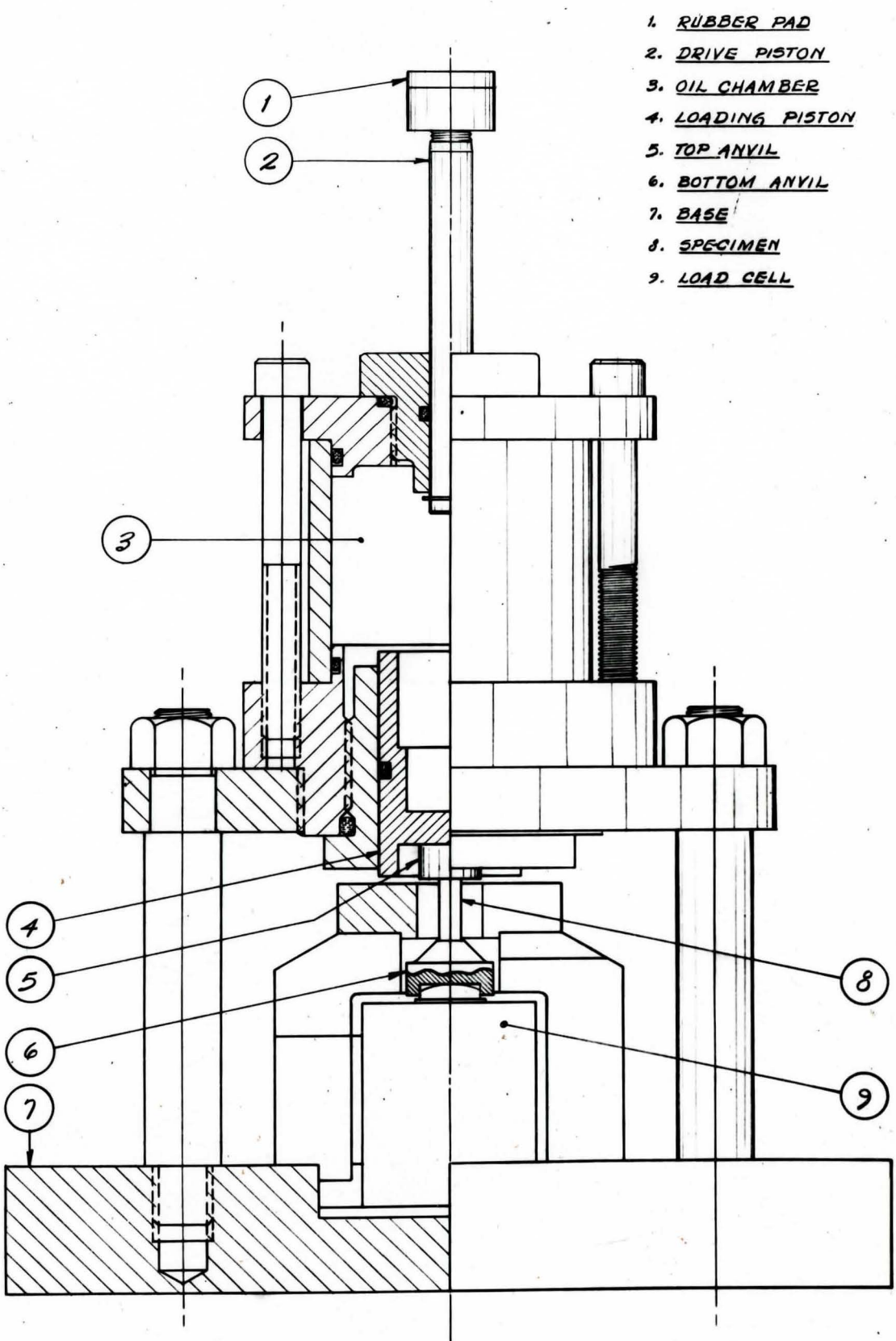

SECTIONAL VIEW OF INTENSIFIER

FIGURE 6

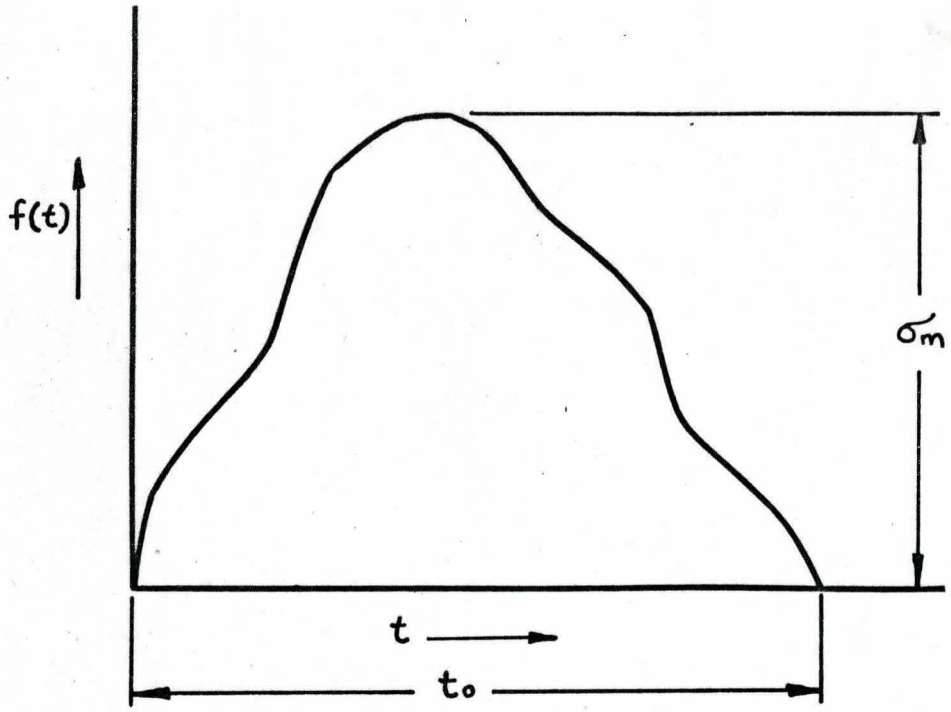

THE GIVEN STRESS FUNCTION

FIGURE 7

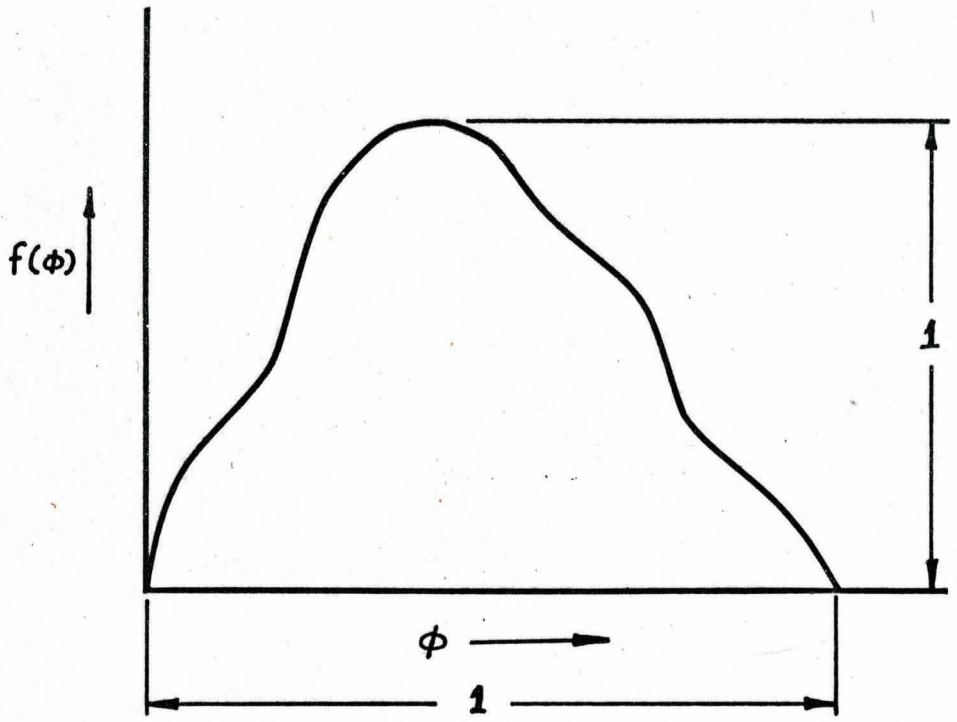

THE STRESS FUNCTION REDUCED TO DIMENSIONLESS PARAMETERS

FIGURE 8

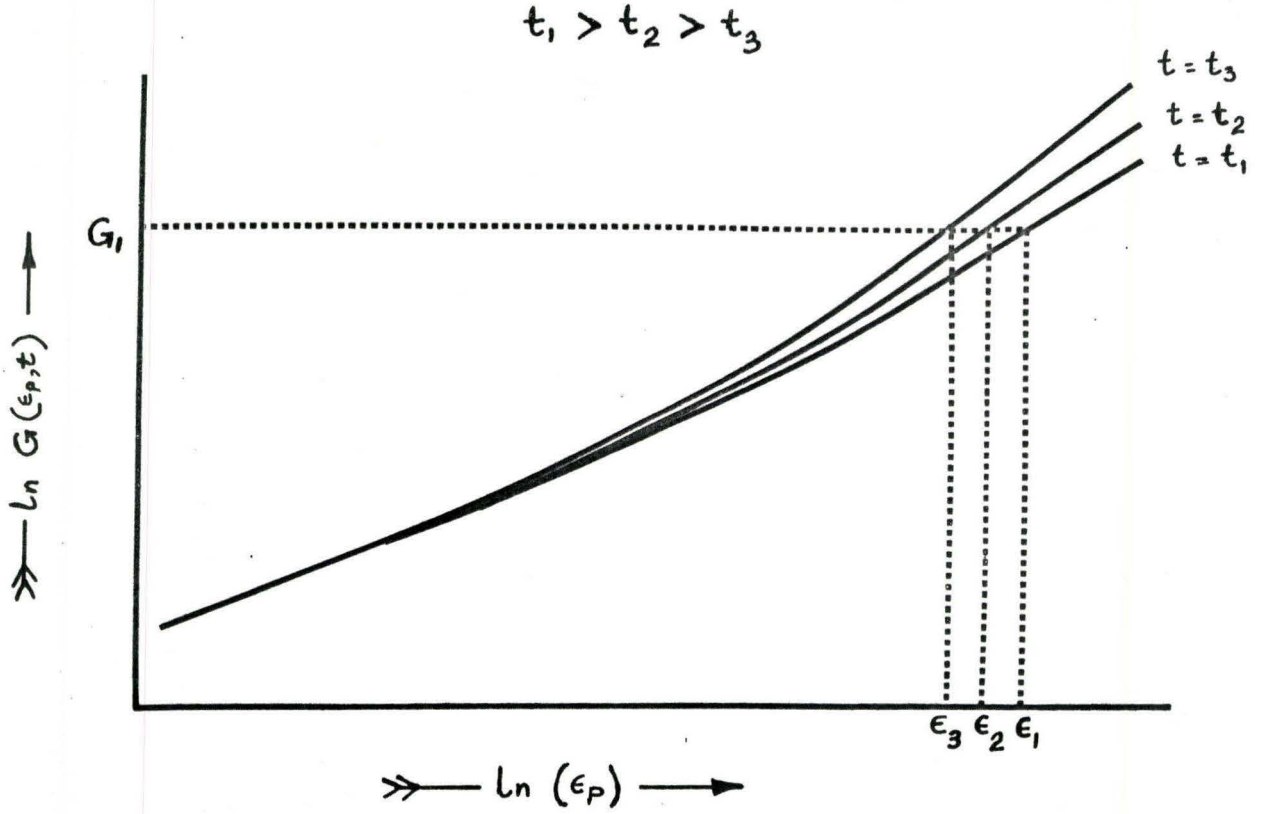

TYPICAL CURVES OF FLOW FUNCTIONS

FIGURE 9

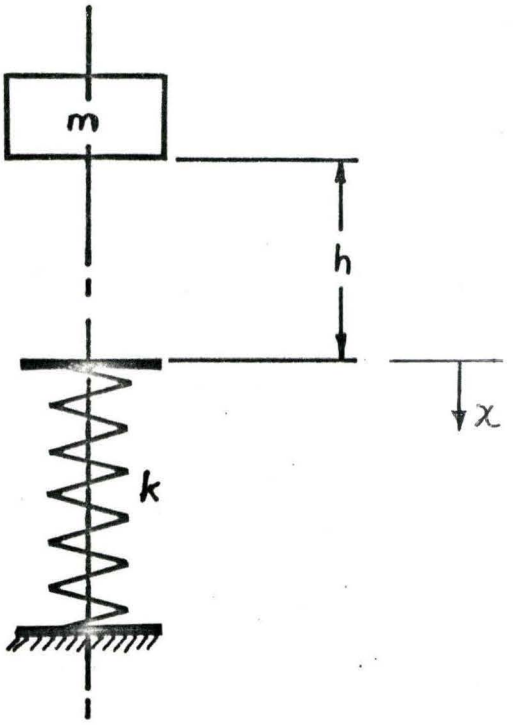

THE SPRING MASS SYSTEM

FIGURE 10

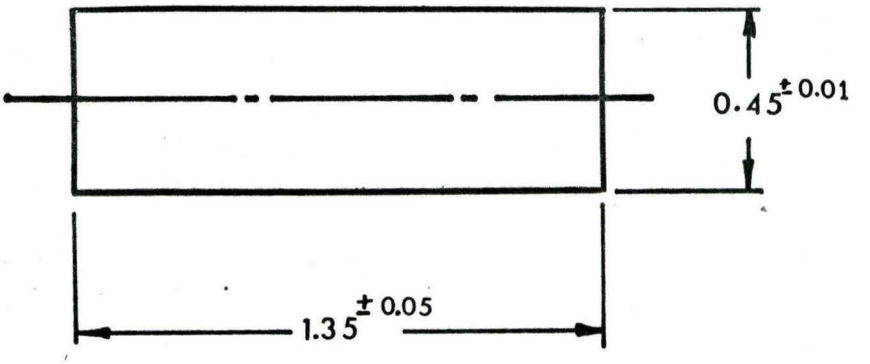

DIMENSIONS OF THE SAMPLES

FIGURE 11

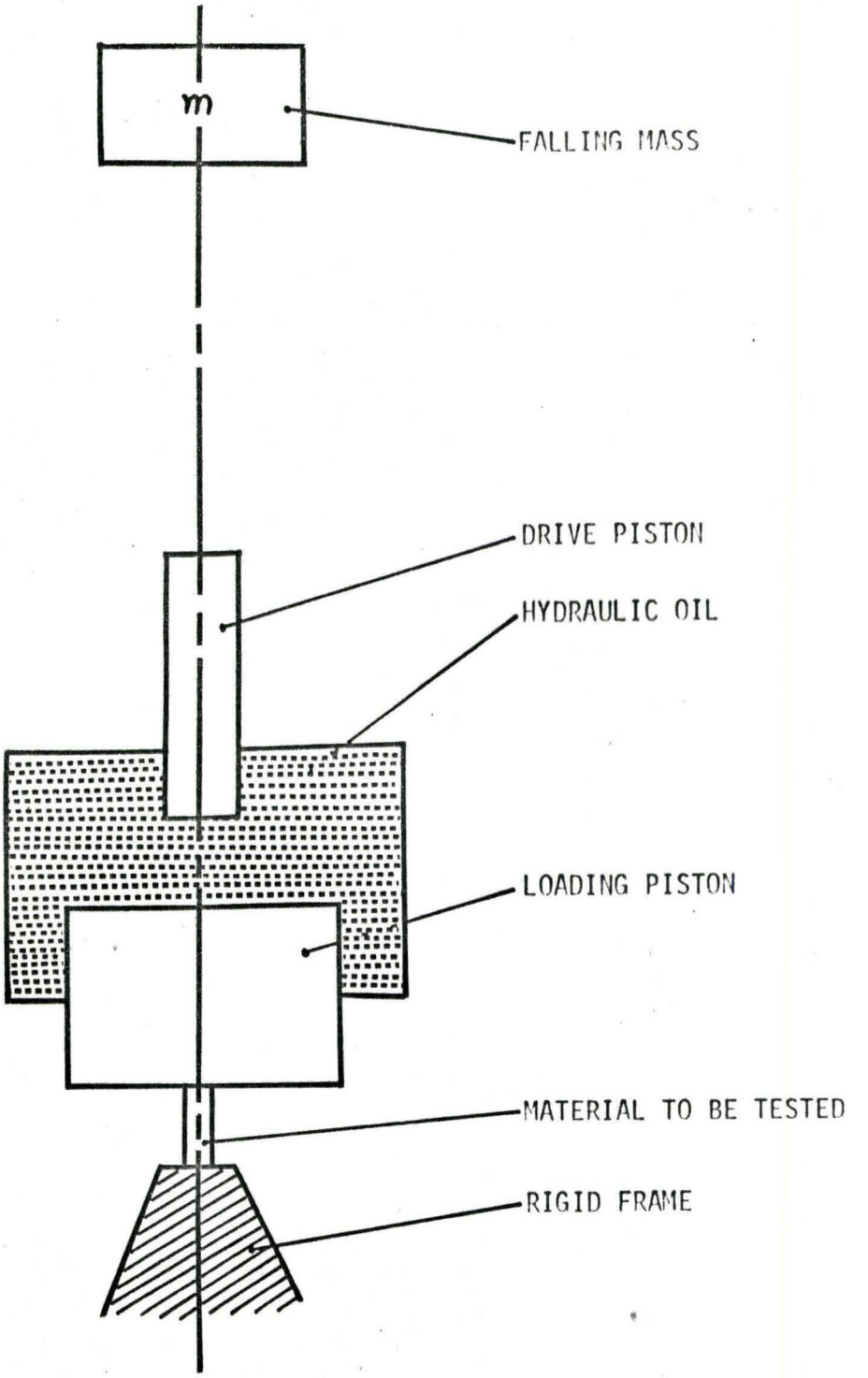

THE PHYSICAL FORM OF SPRING MASS SYSTEM

FIGURE 12

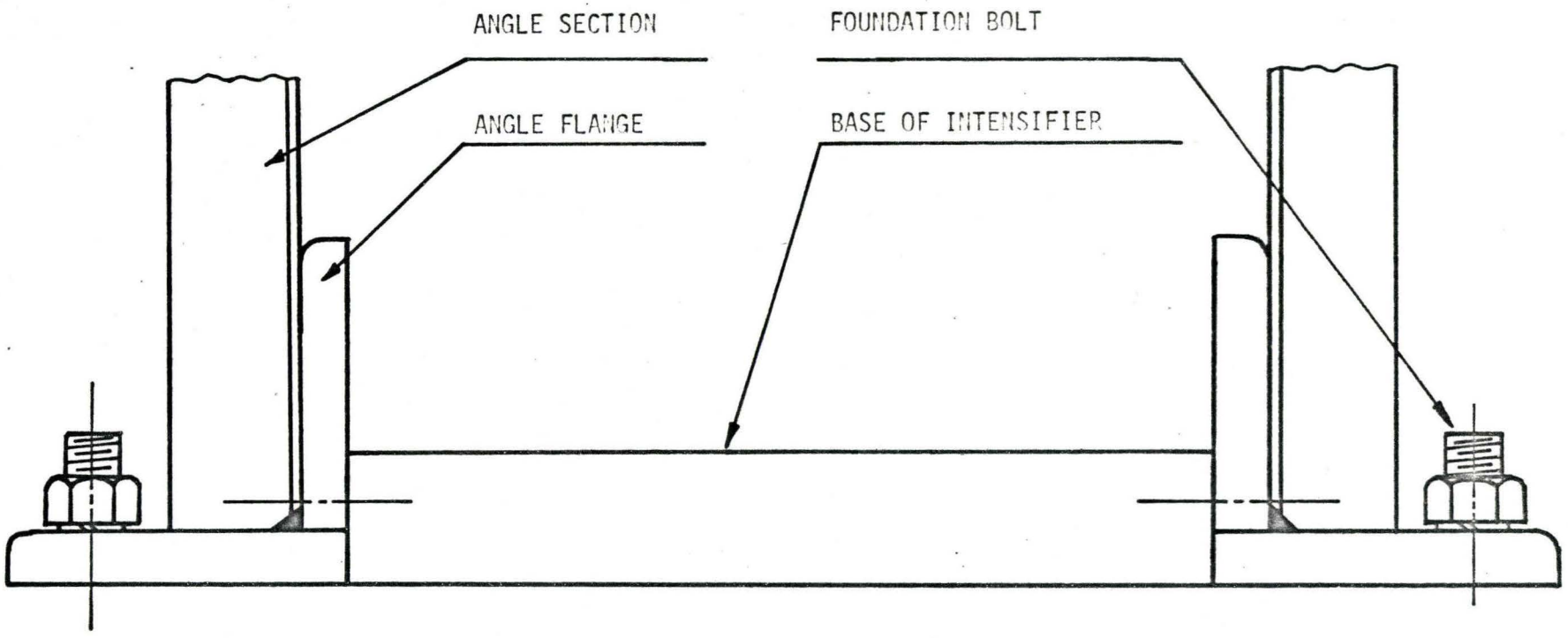

MAIN FRAME FLUSH WITH THE BASE OF THE INTENSIFIER
THROUGH THE ANGLE FLANGES

FIGURE 13

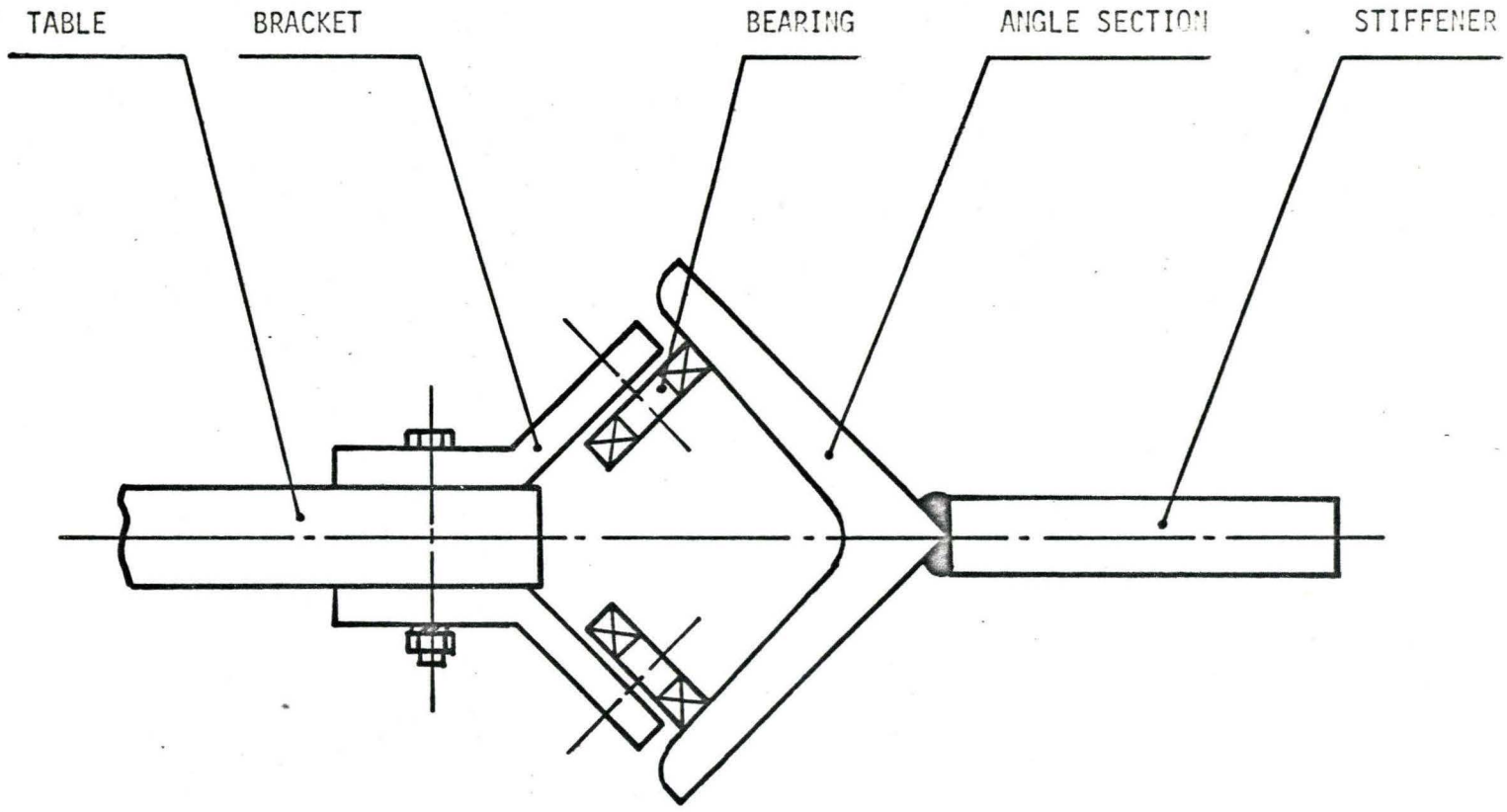

LAY-OUT OF STIFFENERS

The Sketch Also Illustrates The Guiding Arrangement For The Table

FIGURE 14

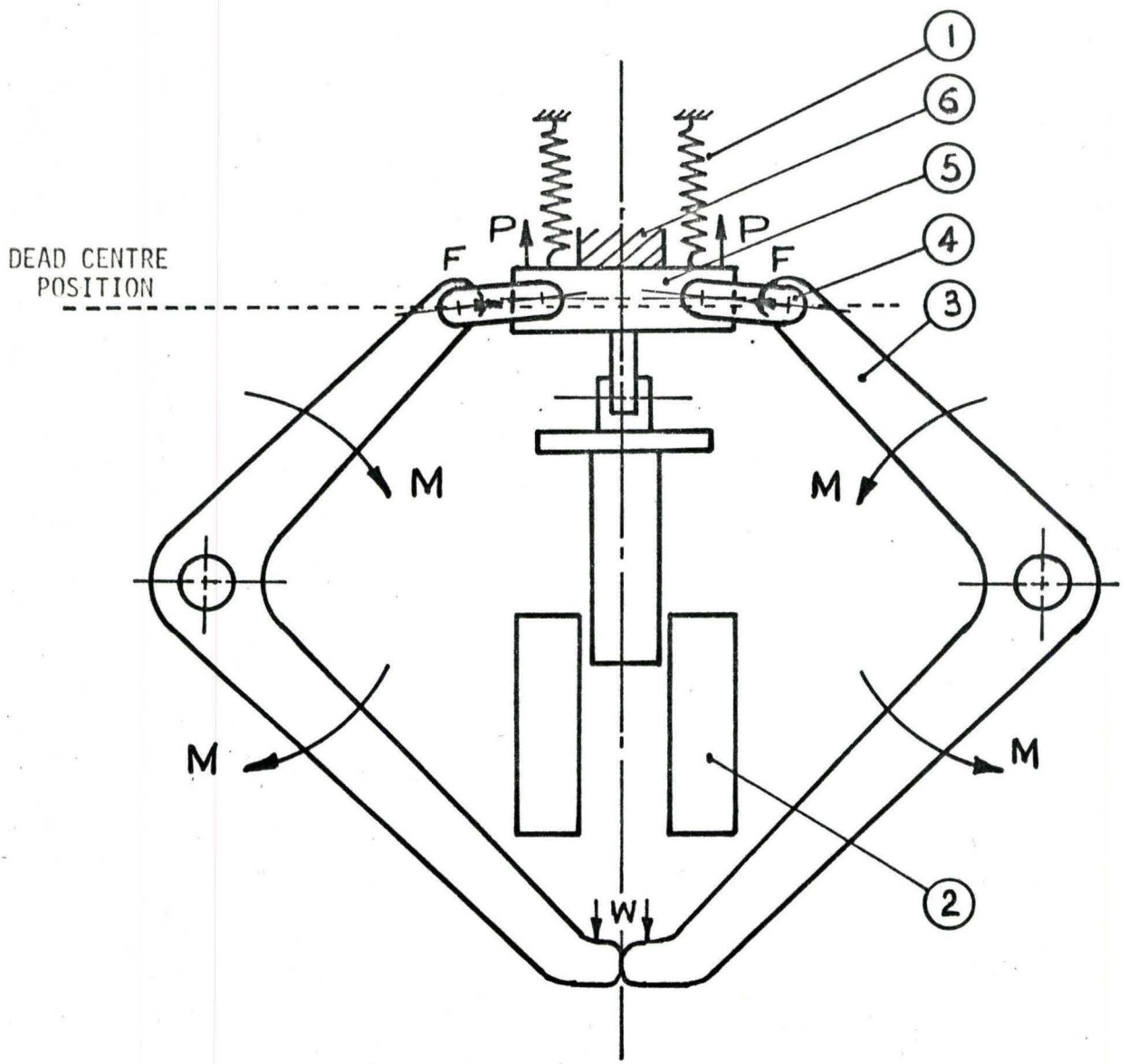

1. Spring
2. Solenoid
3. Main Link
4. Small Link
5. Central Block
6. Stopper

CONFIGURATION OF THE RELEASE MECHANISM
WHEN THE SOLENOID IS NOT ENERGIZED

FIGURE 15

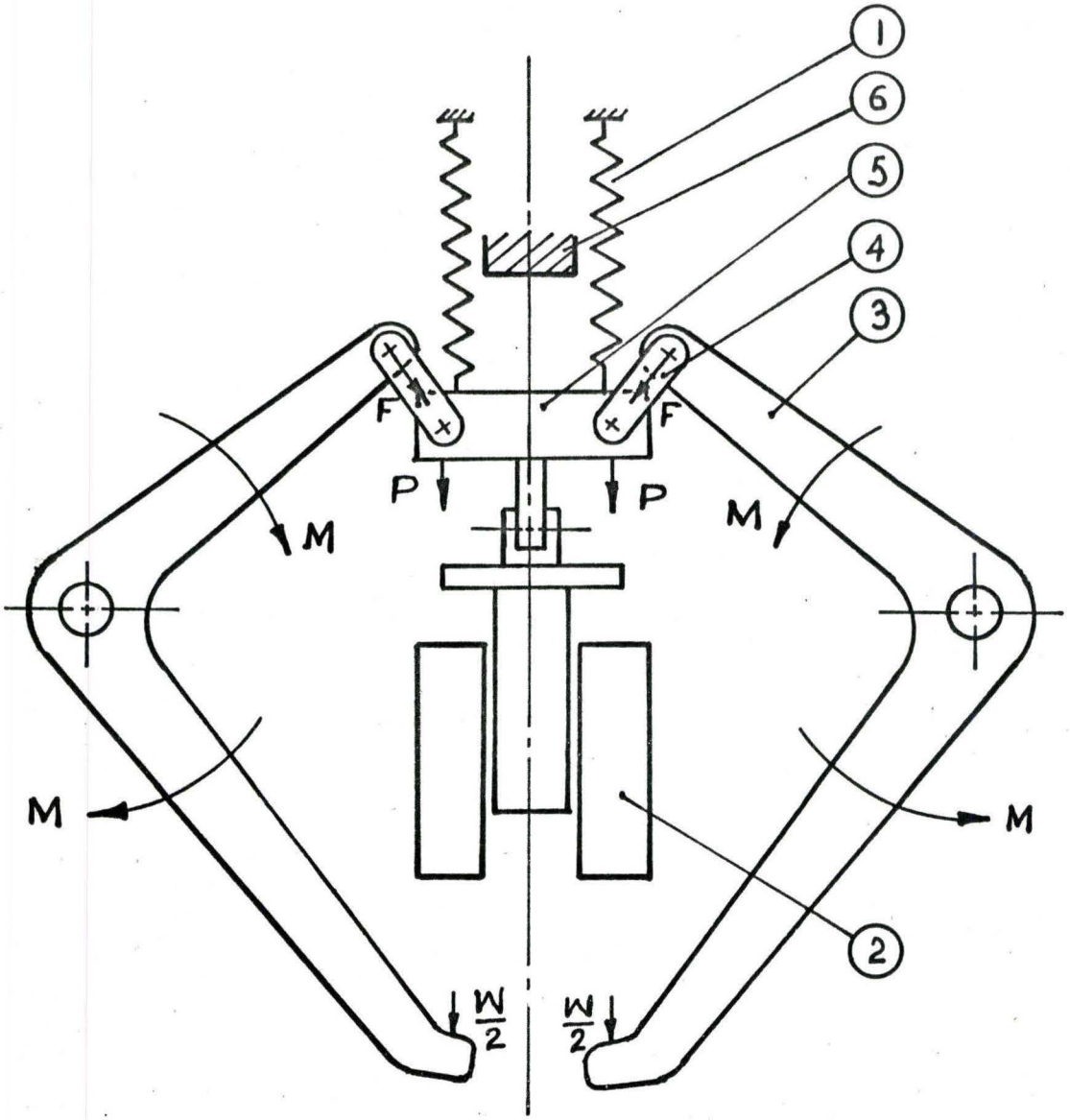

1. Spring
2. Solenoid
3. Main Link
4. Small Link
5. Central Block
6. Stopper

CONFIGURATION OF RELEASE MECHANISM

WHEN THE SOLENOID IS ENERGIZED

FIGURE 16

(a)

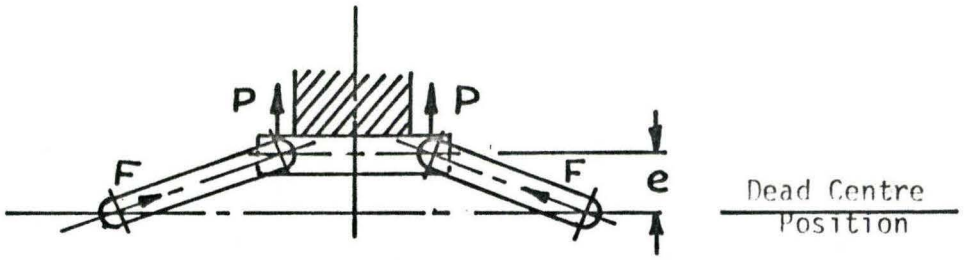

Solenoid is not energized. Central block is above the dead centre position. Force P is acting upwards. Weight of the table is providing the locking force.

(b)

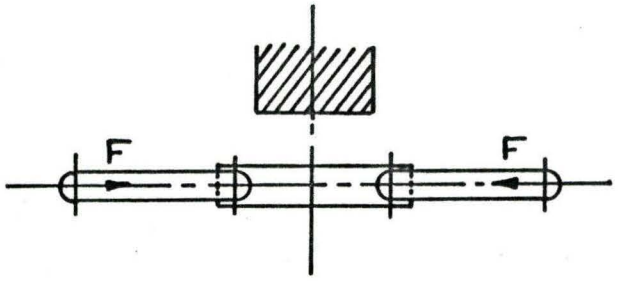

Solenoid has been energized. Central block is on the dead centre position. Force P is zero. Central block will keep moving downwards under the pull exerted by the solenoid. Weight of the table has no influence on the motion of the central block.

(c)

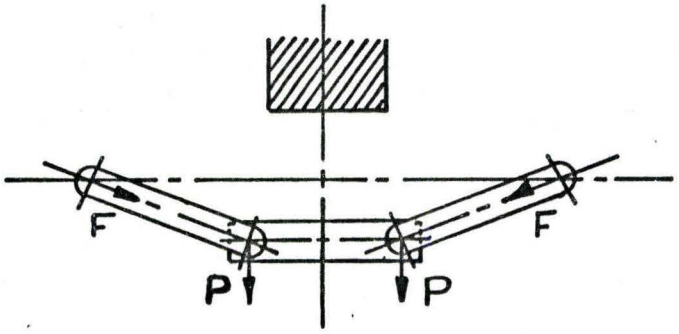

Solenoid is energized. Central block is below the dead centre position. Force P is acting downwards. Weight of the table is helping to open the mechanism

THE RELEASING OPERATION

FIGURE 17

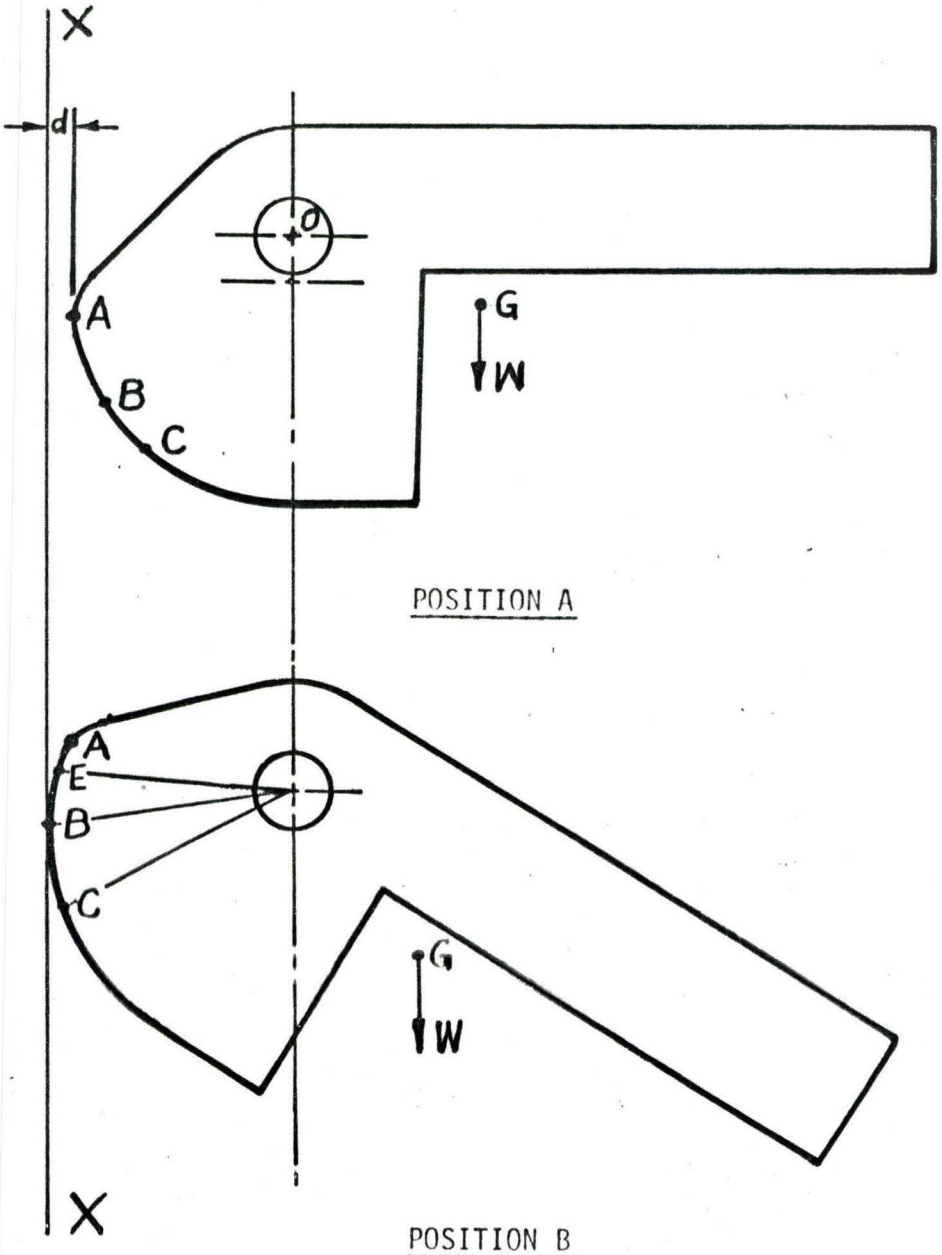

O - Point of Suspension G - Centre of Gravity of Latch

W - Weight of the Latch

X-X - Inner Edge of the Angle Section

d - Clearance Between Latch and the Angle Section

SCHEMATIC REPRESENTATION OF THE WORKING OF THE LATCH

FIGURE 18

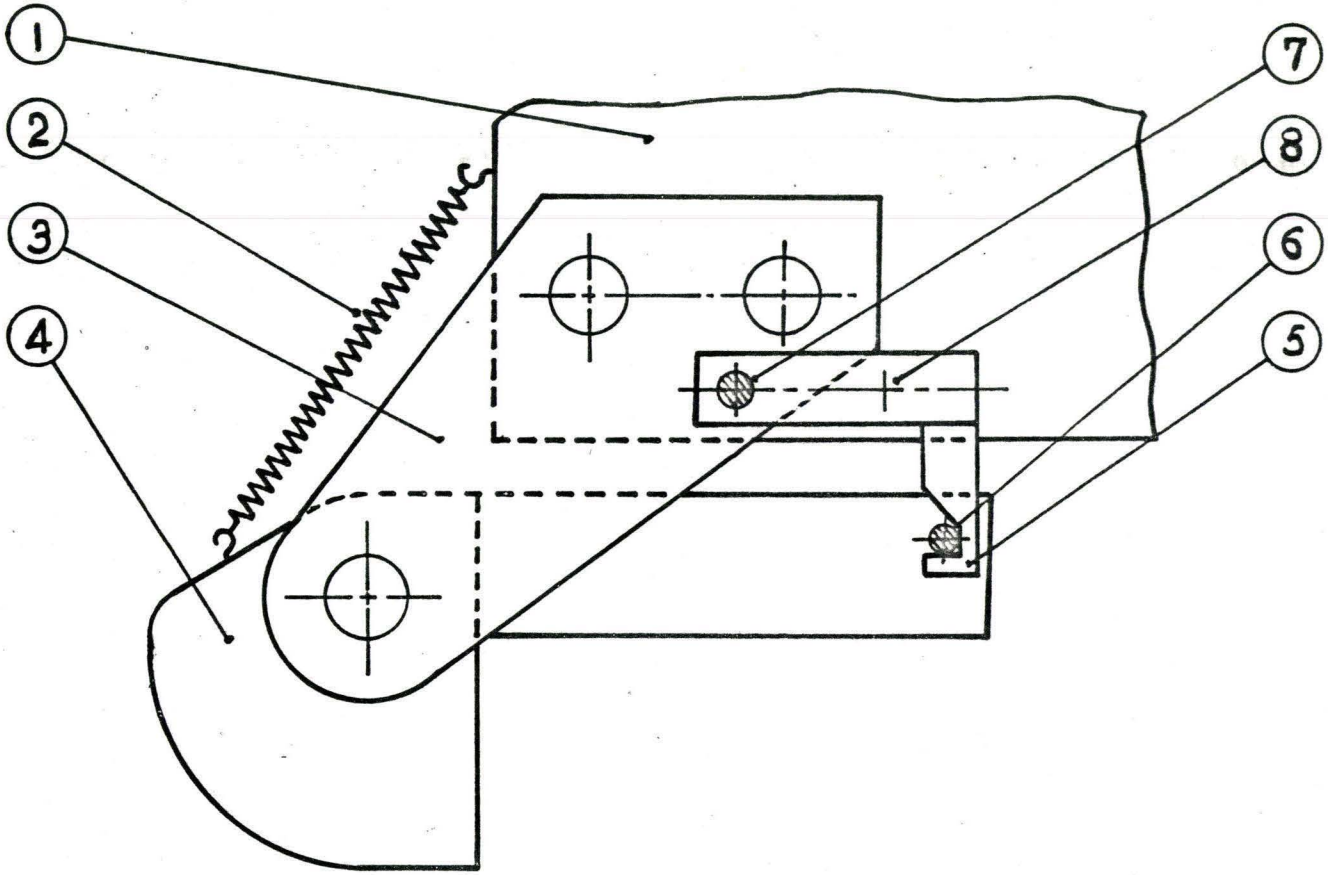

1. Table
2. Bracket
3. Spring
4. Latch
5. Hook
6. Rod - As a Means to hold the Latch
7. Striker
8. Fulcrum

THE LATCH ASSEMBLY

FIGURE 19

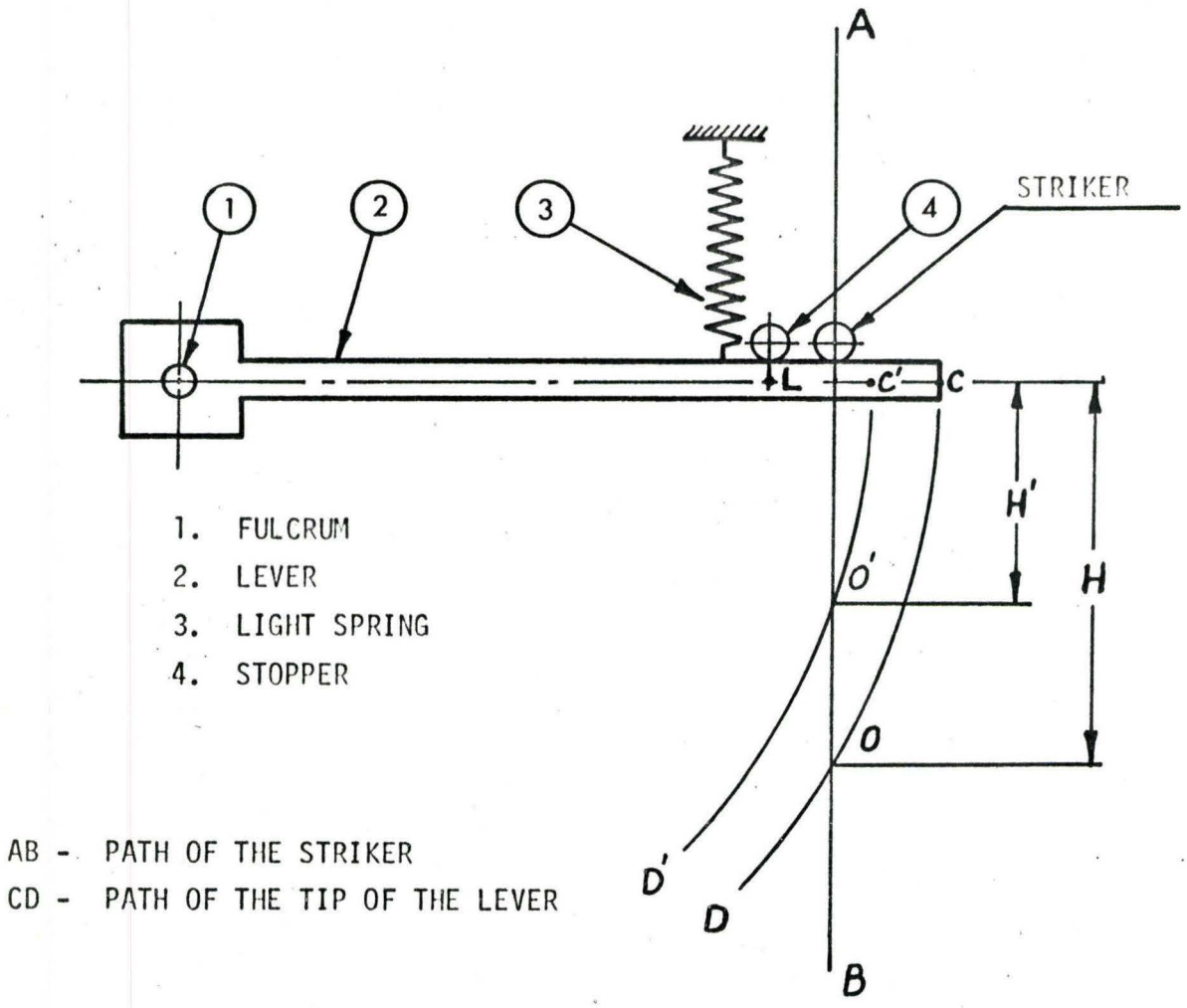

LEVER ASSEMBLY AND ITS OPERATION

FIGURE 20

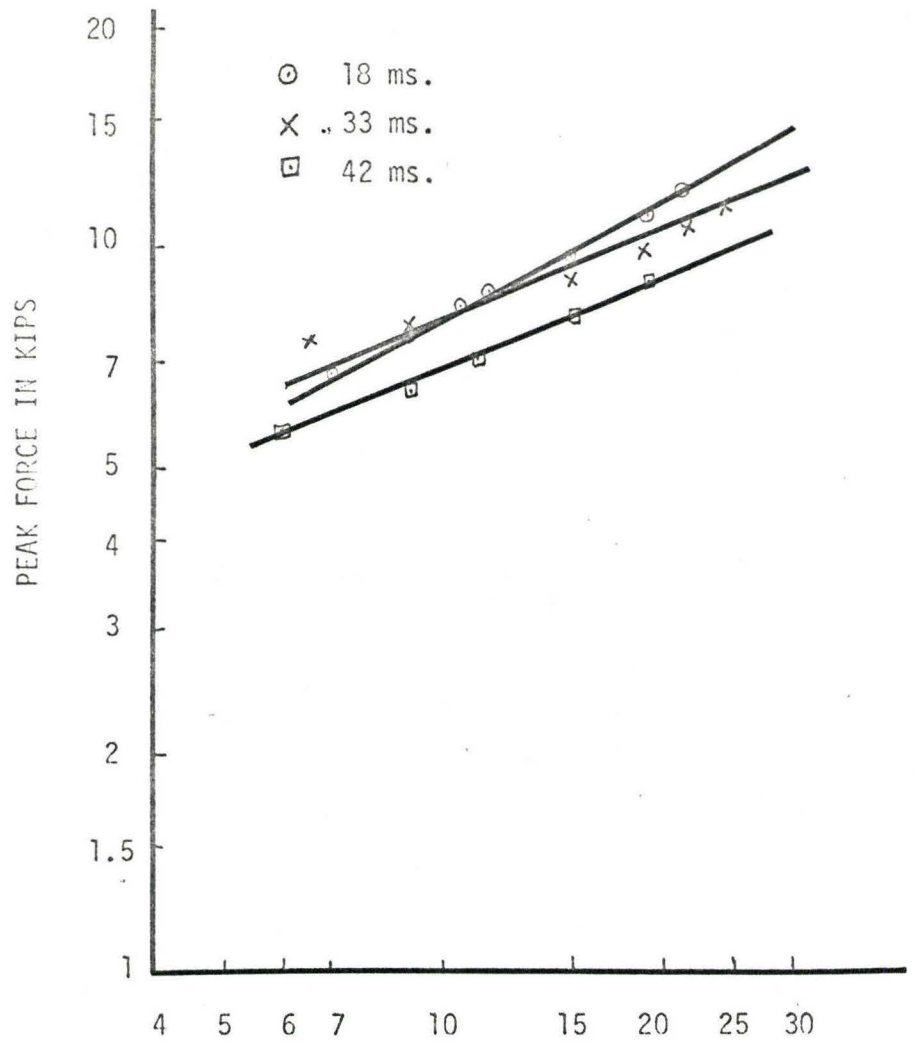

CHARACTERISTIC CURVES

FIGURE 21

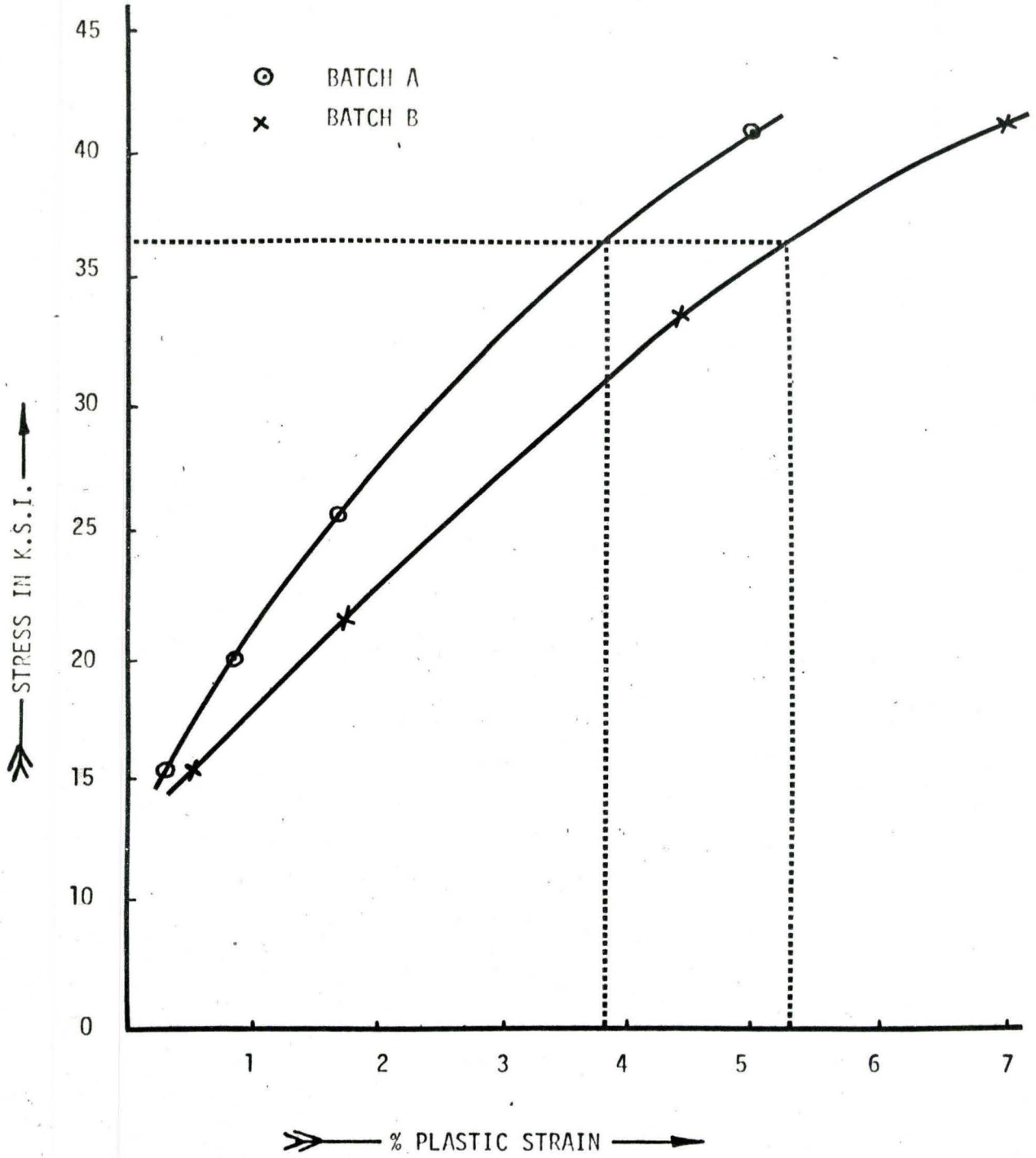

STATIC STRESS-PLASTIC STRAIN RELATIONSHIP

FIGURE 22

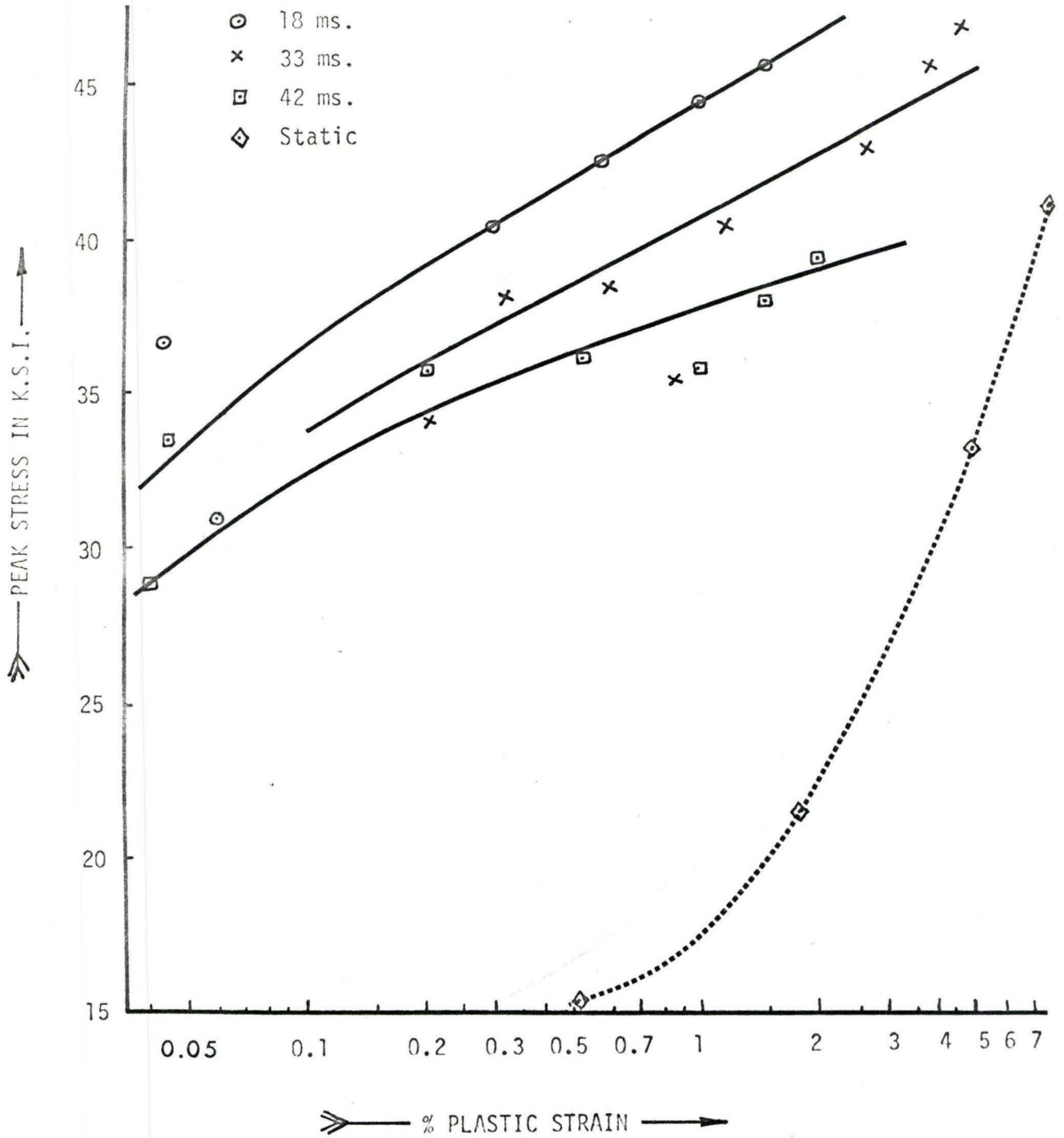

DYNAMIC STRESS-PLASTIC STRAIN RELATIONSHIP-BATCH B

FIGURE 23

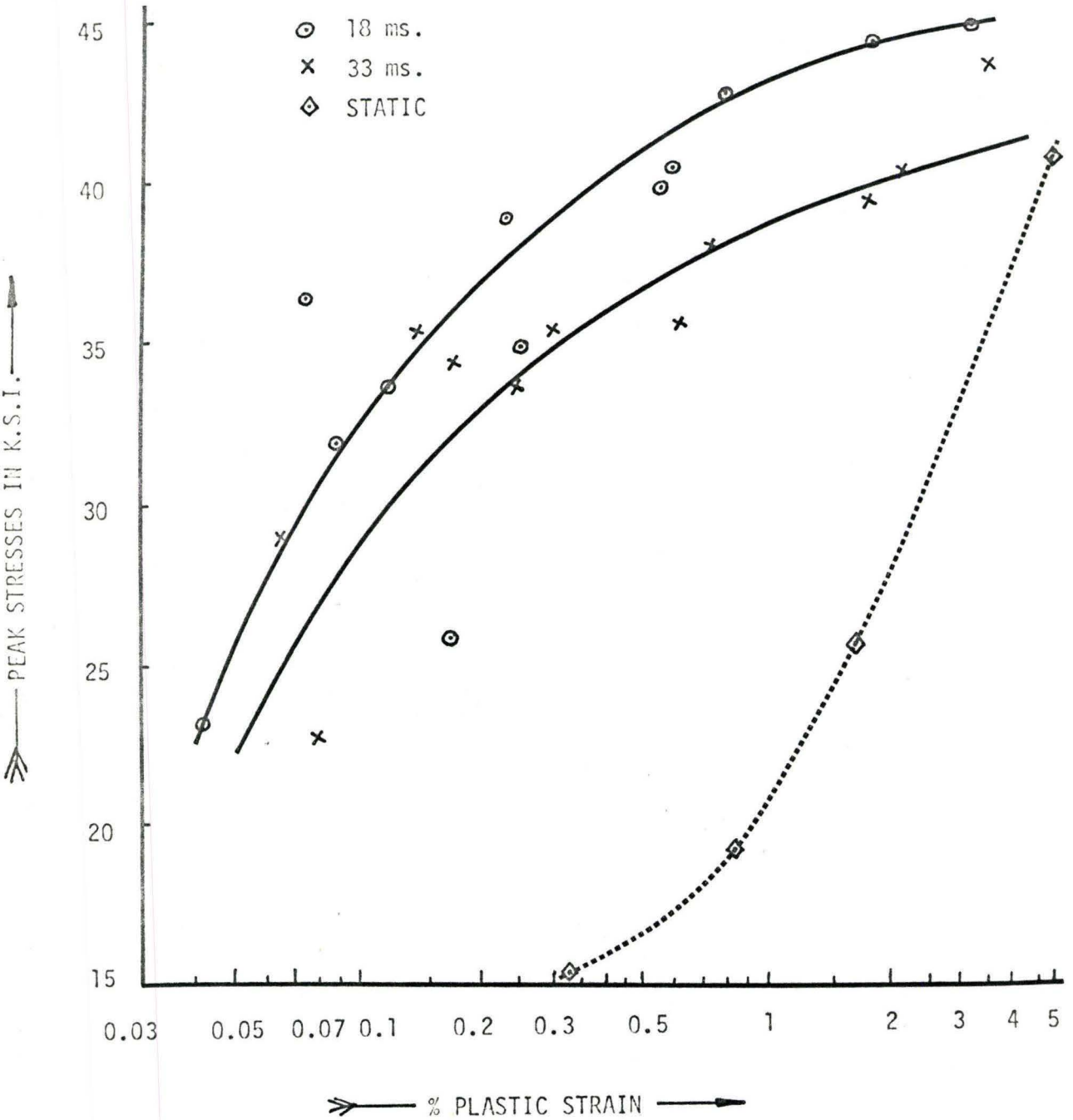

DYNAMIC STRESS-PLASTIC STRAIN RELATIONSHIP - BATCH A

FIGURE 24

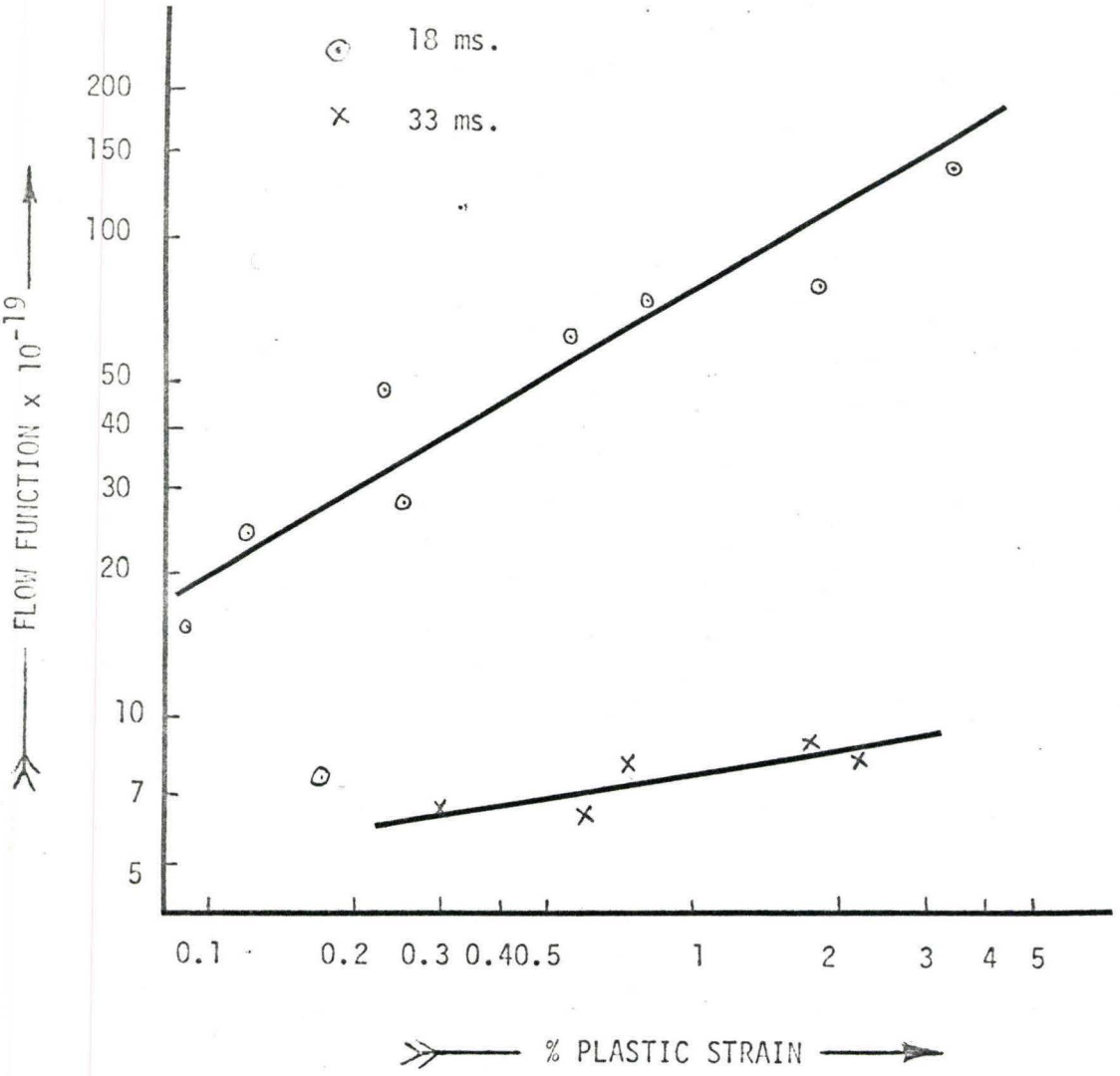

FLOW FUNCTION VERSUS PLASTIC STRAIN

BATCH - A

FIGURE 25

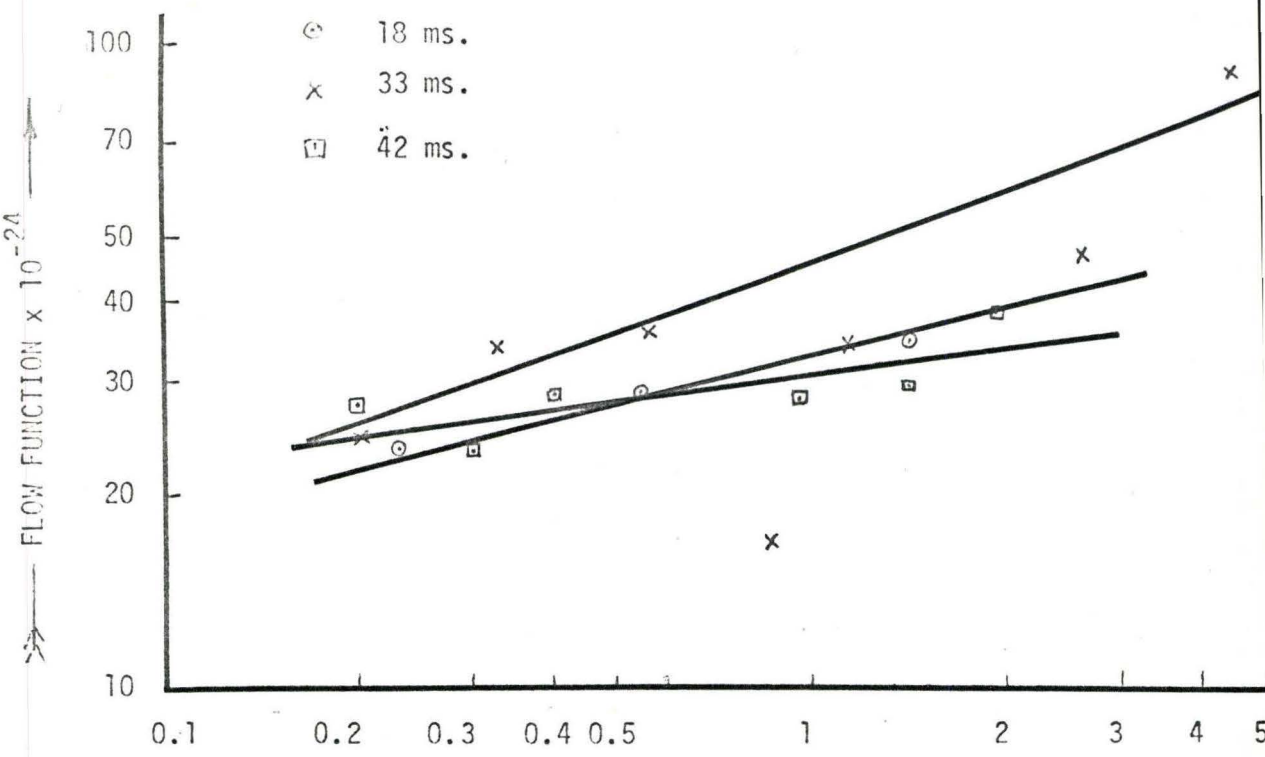

FLOW FUNCTION VERSUS PLASTIC STRAIN

BATCH - B

FIGURE 26

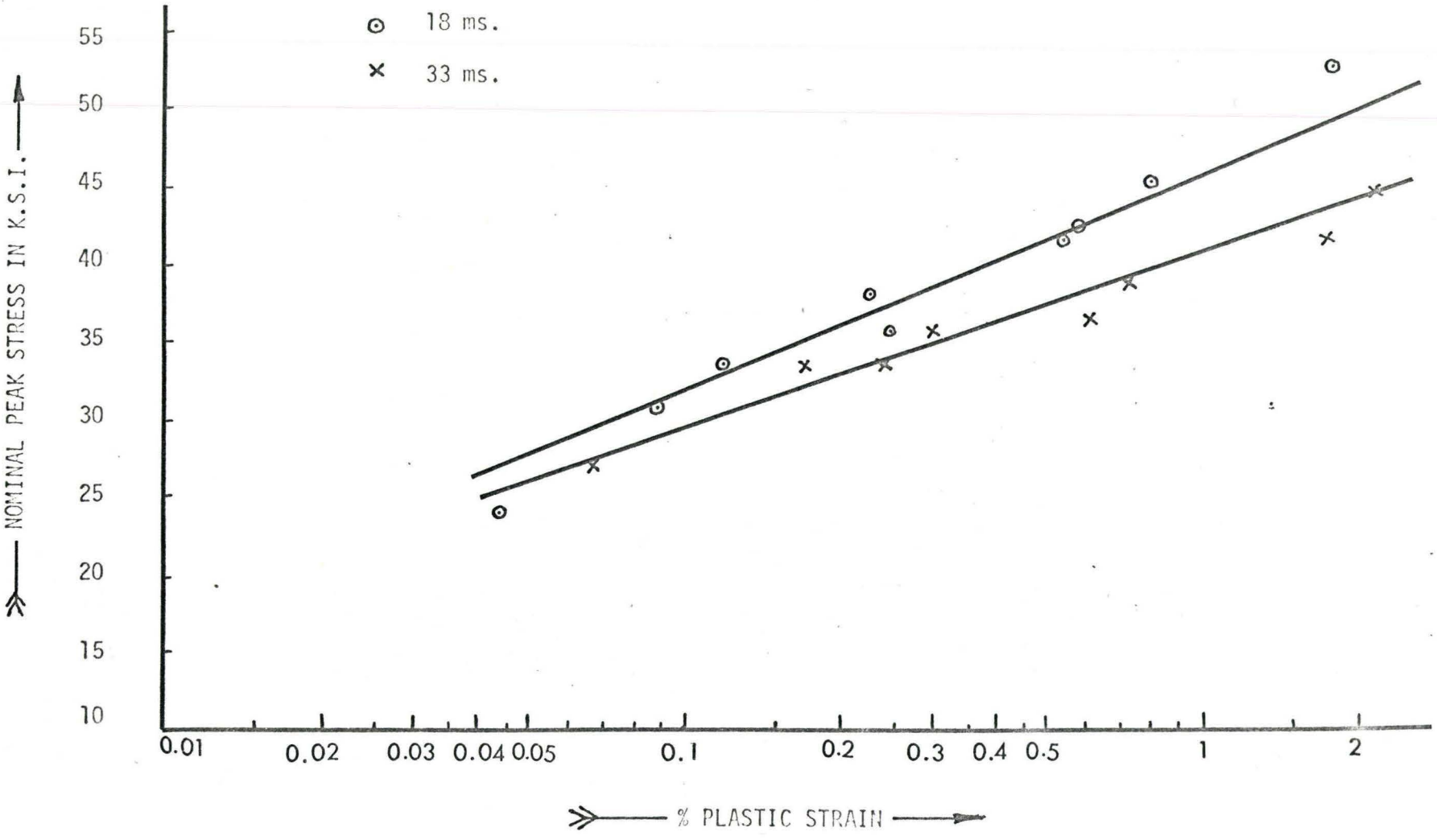

NOMINAL PEAK STRESS VERSUS PLASTIC STRAIN - BATCH A

FIGURE 27

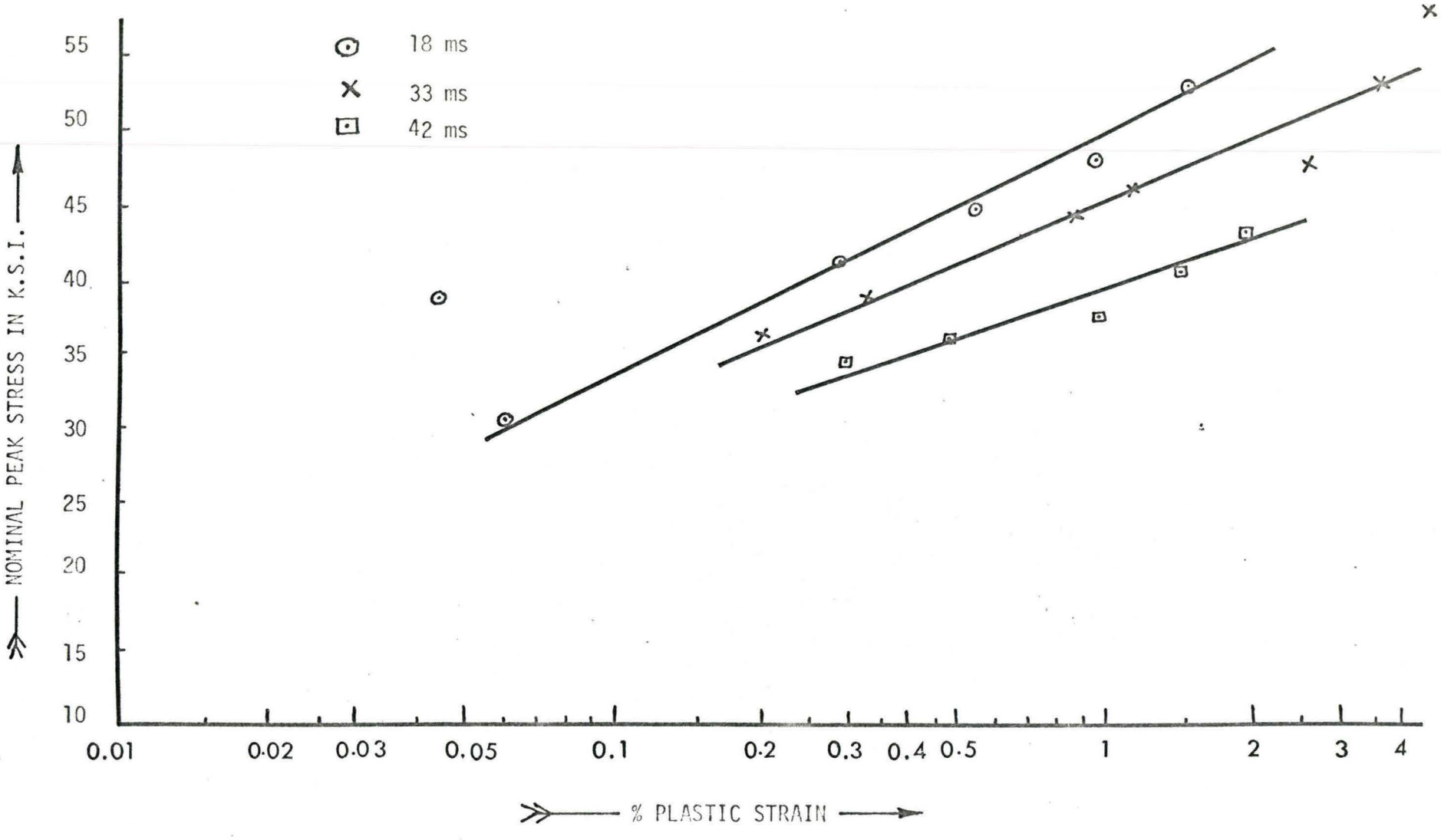

NOMINAL PEAK STRESS VERSUS PLASTIC STRAIN - BATCH B

FIGURE 28

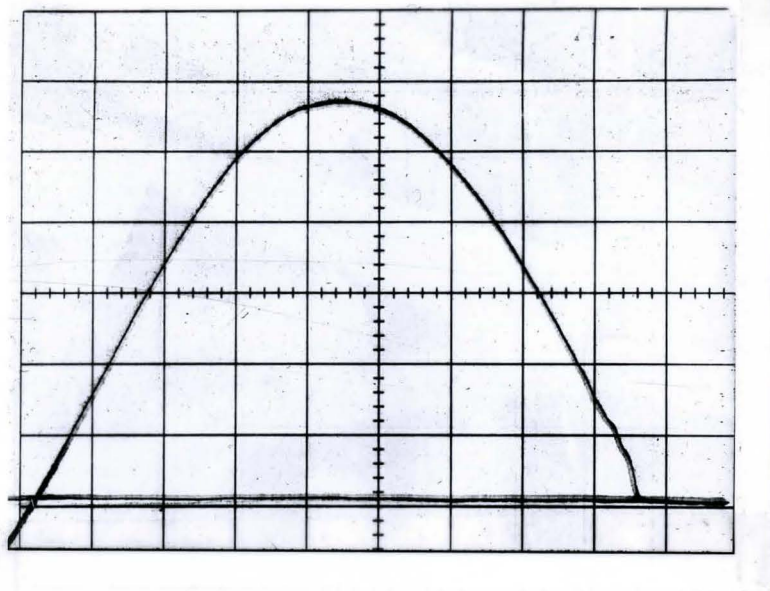

A TYPICAL LOAD PULSE GENERATED BY THE SYSTEM

FIGURE 29

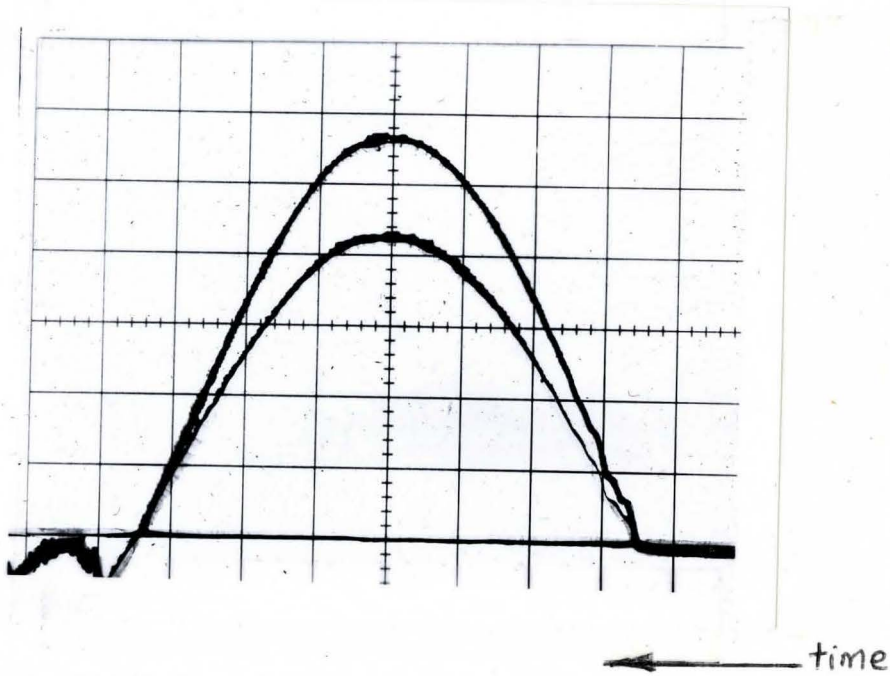

TWO TRACES SUPERIMPOSED ON EACH OTHER SHOWING THAT THE DURATION OF LOADING IS INDEPENDENT OF THE HEIGHT OF DROP

FIGURE 30

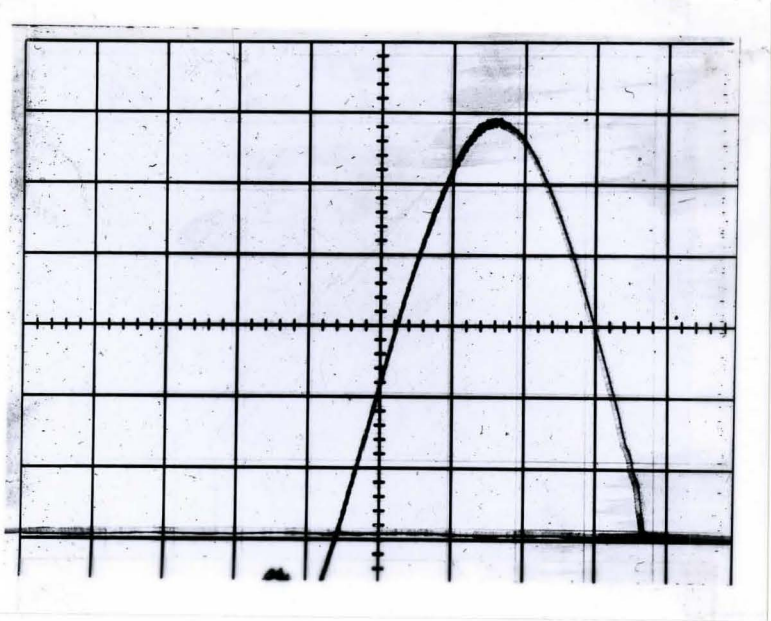

time

A TRACE SHOWING VERY LITTLE YIELD OF THE MATERIAL

FIGURE 31

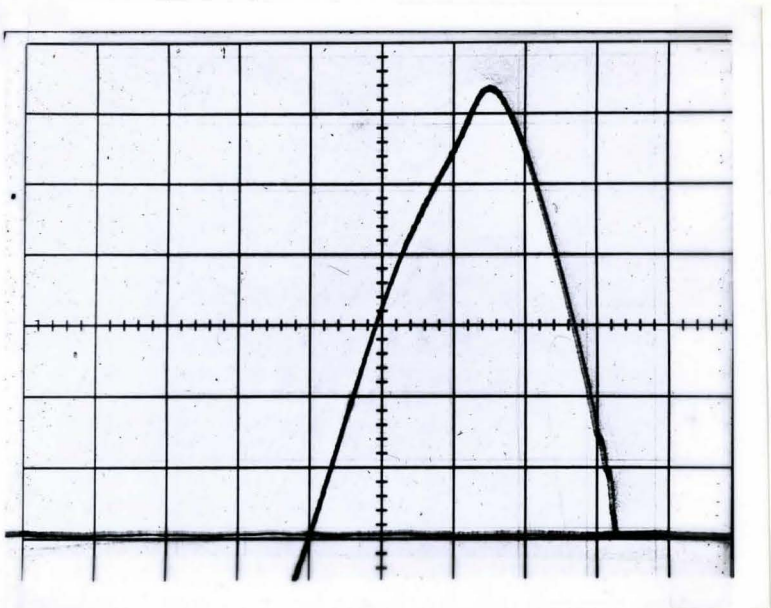

time

A TRACE SHOWING APPARENT YIELD

FIGURE 32

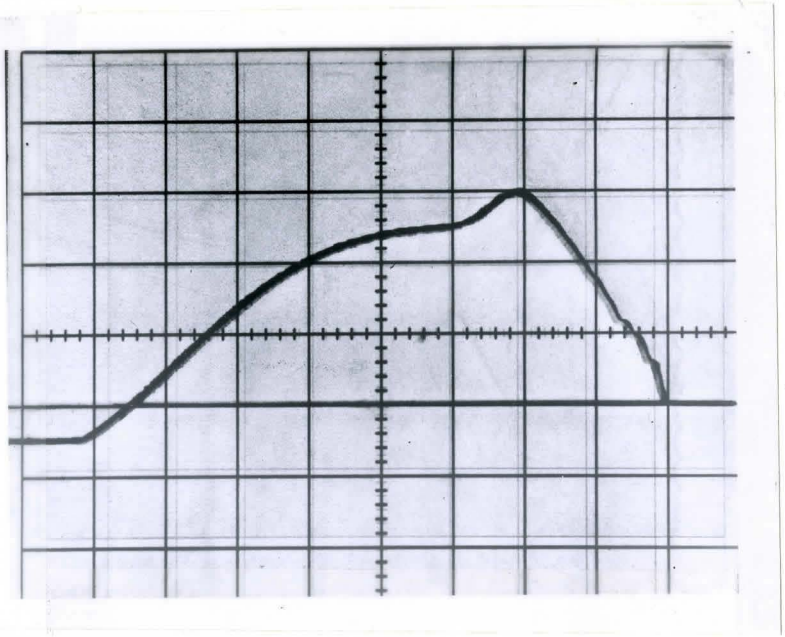

A TRACE SHOWING LARGE AMOUNT OF YIELD

Note the increase in the duration of loading

FIGURE 33

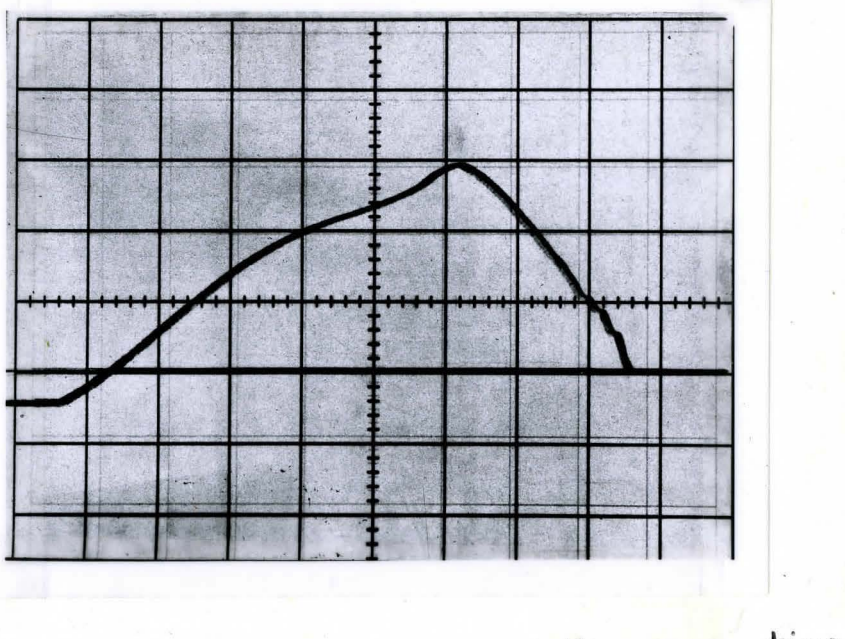

A TRACE SHOWING LARGE AMOUNT OF YIELD

Note the increase in the duration of loading

FIGURE 34

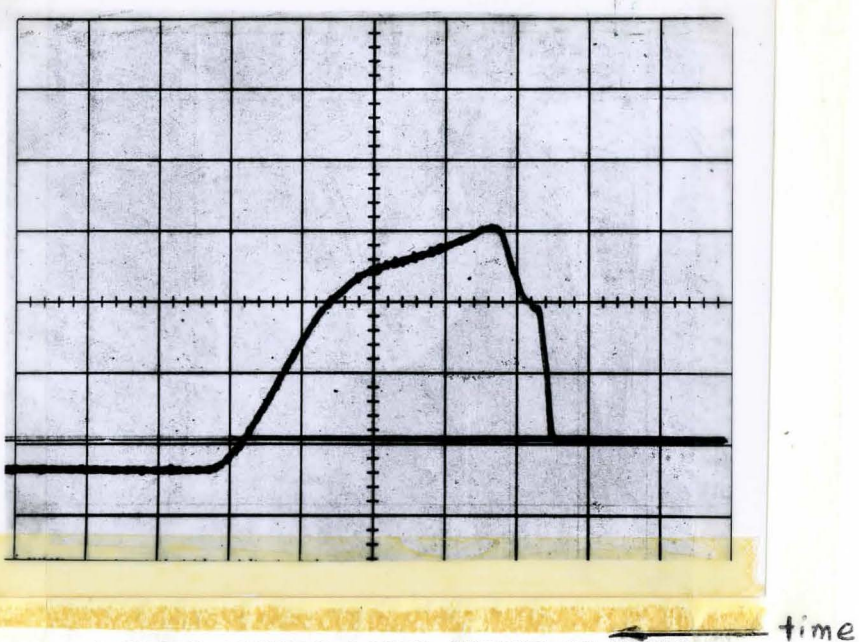

A TRACE SHOWING LARGE AMOUNT OF YIELD

Note the flattening of the stress-pulse

FIGURE 35

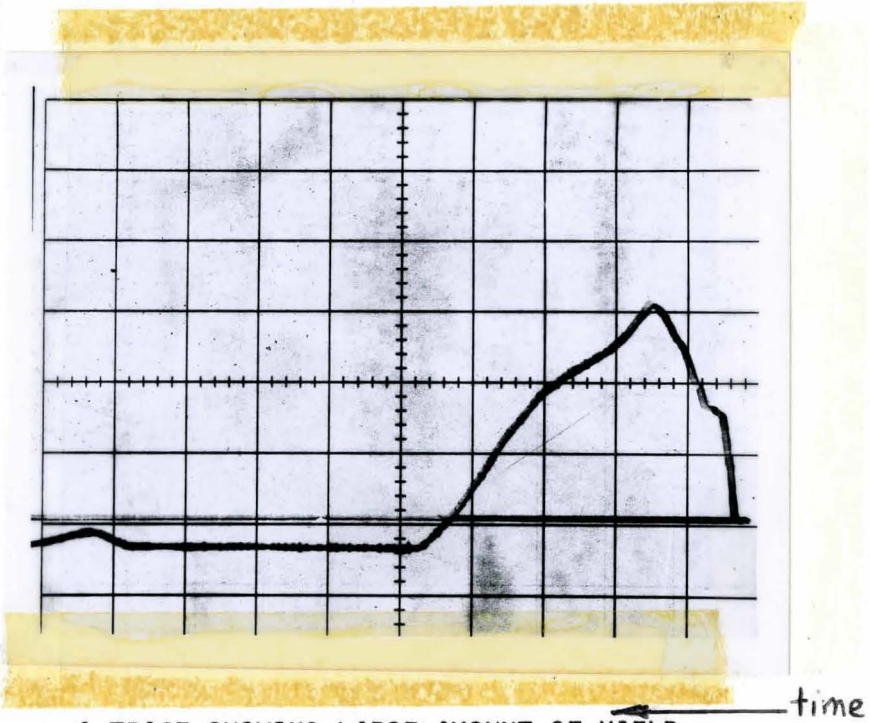

A TRACE SHOWING LARGE AMOUNT OF YIELD

Note the flattening of the stress-pulse

FIGURE 36

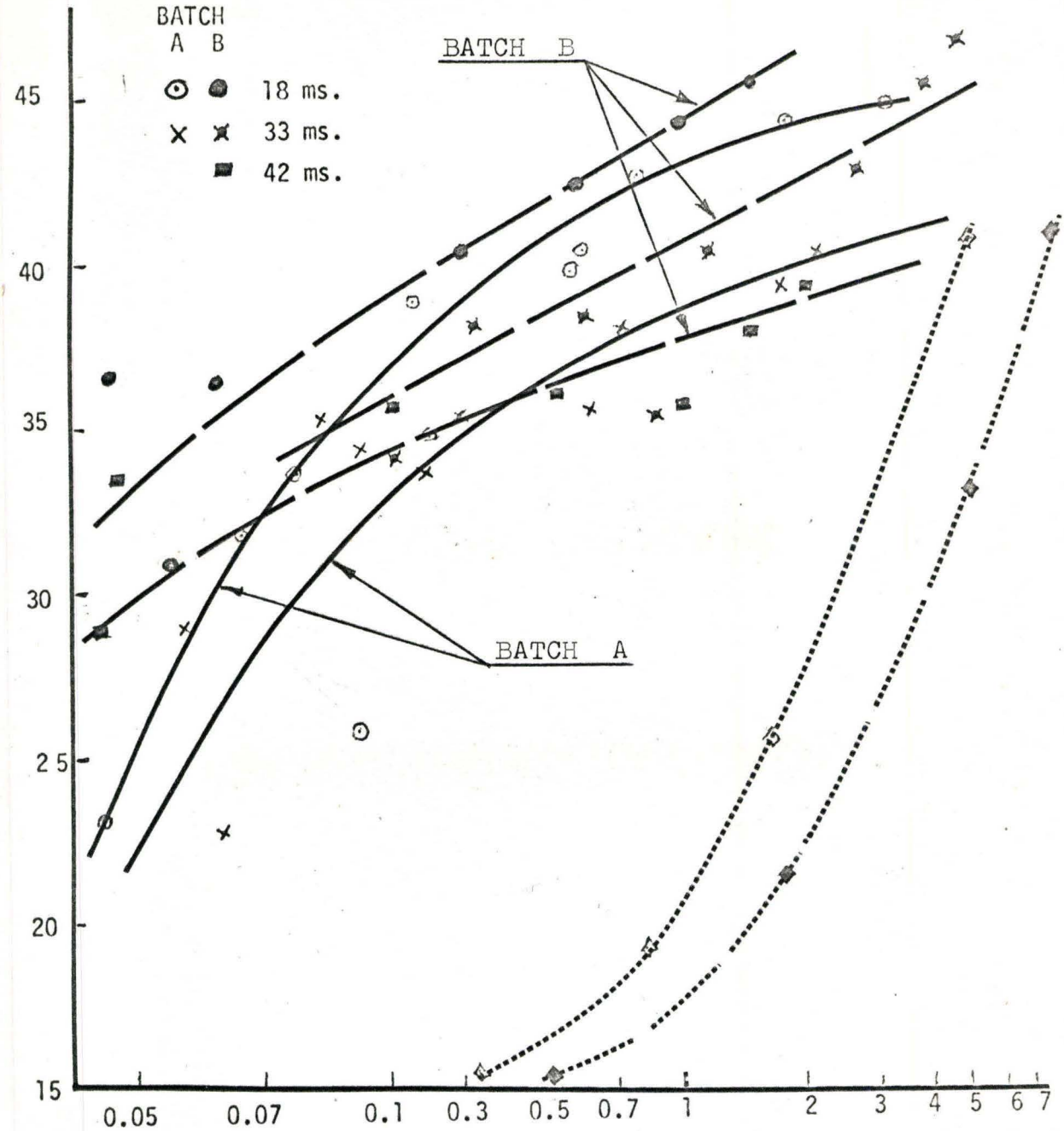

COMPARISON OF BATCH A AND BATCH B FOR SENSITIVITY TO STRAIN RATES

FIGURE 37